

SYNTHESIS AND CHARACTERIZATION OF CATALYSTS USED FOR THE PETROCHEMICAL INDUSTRY



By

SUNDUS FATIMA

**School of Chemical and Materials Engineering (SCME)
National University of Sciences and Technology (NUST)**

2012

SYNTHESIS AND CHARACTERIZATION OF CATALYSTS USED FOR THE PETROCHEMICAL INDUSTRY



Name

Sundus Fatima

Reg. No

2010-NUST-MS PhD-EM-E-15

**This work is submitted as a MS thesis in partial fulfillment of the requirement
for the degree of
(MS in Energetic Materials Engineering)**

Supervisor Name: Dr. Shaneela Nosheen

**School of Chemical and Materials Engineering (SCME)
National University of Sciences and Technology (NUST),
H-12 Islamabad, Pakistan
December, 2012**

Certificate

This is to certify that work in this thesis has been carried out by **Ms. Sundus Fatima** and completed under my supervision in in School of Chemical and Materials Engineering, National University of Sciences and Technology, H-12, Islamabad, Pakistan.

Co-supervisor _____

Dr. Muahammad Mujahid

Principial

School of Chemical and Materials Engineering
National University of Sciences andTechnology,
Islamabad

Supervisor: _____

Dr. Shaneela Nosheen

Associate Professor

School of Chemical and Materials Engineering
National University of Sciences andTechnology,
Islamabad

Submitted through

Principal/Dean,

School of Chemical and Materials Engineering

National University of Sciences andTechnology, Islamabad

Dedication

To humanity.....

“The things that will destroy us are: politics without principle; pleasure without conscience; wealth without work; knowledge without character; business without morality; science without humanity; and worship without sacrifice. – Mahatma Gandhi”

Acknowledgement

Foremost, I would like to express my sincerest gratitude to my supervisor Dr. Shaneela Nosheen for her incessant support, serenity, motivation, enthusiasm, and immense knowledge. Her guidance helped me at the time of research and writing of this thesis. I could not have imagined having a better advisor and mentor for my MS research project.

I would like to thank my co-supervisor, Dr Muhammad Mujahid. He has always been very kind to me.

I must thank Dr. Zafar-uz-zaman for agreeing to be my external thesis examiner. He gave very valuable suggestions and insightful comments.

I would like to thank the rest of my thesis committee: Dr. Arshad Hussain, Dr. Muhammad Shahid, and Dr. Abdul Qadeer Malik, for their encouragement, insightful comments, and hard questions.

I would like to thank the Incharge Chemistry Lab; Dr. Habib Nasir, for his support, guidance, and patience throughout the synthesis period.

I would like to thank Dr. Amir Habib for his generous contribution.

I must also thank the SCME Laboratories' staff for helping me with the use of new or unfamiliar equipments.

Last but not the least; I would like to thank the Assistant Librarian, Mrs. Saira, for her bighearted favor in using SCME library during my MS study and literature survey for this project.

Abstract

Nanocrystalline zeolite type catalysts gobbinsite zeolite (Na-P1) and Dachiardite-Na (DAC-Na) were synthesized in round bottom flask with total reflux at lower temperature (below 100°C) under constant stirring. Silica gel and tetraethylorthosilicate (TEOS) were used as silica source for Na-P1 and DAC-Na synthesis respectively. Sodium aluminate (NaAlO_2) was used as Alumina source for both types of zeolite synthesis. Both products were characterized by using various analytical techniques such as X-ray Diffraction (XRD), Scanning Electron Microscope (SEM), Atomic Force Microscopy (AFM) and Fourier Transform Infrared (FT-IR) analysis. Thermogravimetric study of Thermal and Catalytic pyrolysis of LDPE was briefly discussed to understand the catalytic activity of both catalysts.

Table of Contents

Chapter 1: Introduction	1
1.1 Background	1
1.2 An Introduction to Petrochemical Industry	2
1.3 History of Catalysis in Petrochemical Industry	4
Chapter 2: Literature review	5
2.1 Introduction	5
2.2 Crystalline Microporous Materials: Zeolites	5
2.3 Discovery and Applications	5
2.4 Zeolite Structure	6
2.5 Synthesis of Zeolites	9
2.6 Zeolitic Catalysis Mechanism	14
2.7 Nanostructured Zeolites	15
2.8 Zeolite synthesis steps	16
2.9 Synthesis of Na-P1	17
2.10 Synthesis of DAC-Na	18
2.11 Characterization	19
2.12 LDPE Pyrolysis	20
Chapter 3: Experimental	22
3.1 Synthesis of NaP1	22
3.2 Synthesis of DAC-Na	24
Chapter 4: Results and Discussion	26
4.1.1 XRD for Na-P1 Zeolite	26
4.1.2 XRD for DAC-Na zeolite	27
4.2.1 SEM Analysis for Na-P1	28
4.2.2 SEM Analysis for DAC-Na	30
4.3.1 AFM Analysis for Na-P1	32
4.3.2 AFM Analysis for DAC-Na	33
4.4 FT-IR Analysis	34
Chapter 5: Application	35
5.1 Thermogravimetric Study of LDPE Pyrolysis with Na-P1	35
5.2 Thermogravimetric Study of LDPE Pyrolysis with DAC-Na	36
Chapter 6: Future work	38
Chapter 7: Conclusion	39
References	40

List of Tables

Table 1.1: Origin of petrochemicals

Table 2.1: Zeolite topic of research for decades

Table 2.2: Effect of heteroatoms for Zeolite synthesis

Table 4.1: NaP1 XRD assignments

Table 4.2: DAC-Na XRD assignments

Table 5.1: Thermogravimetric study of LDPE pyrolysis with NaP1

Table 5.2: Thermogravimetric study of LDPE pyrolysis with NaP1

List of Figures

- Figure 1.1: Comparison of chemical reaction with and without catalyst.
- Figure 1.2: Impact of catalysis in Process Industry
- Figure 1.3: Chemical Industry products
- Figure 2.1: Zeolitic structure buildup
- Figure 2.2: A schematic 8 membered zeolitic ring
- Figure 2.3: subunits of zeolite structure
- Figure 2.4: DAC type Dachiardite zeolites' framework
- Figure 2.5: GIS type materials conformation
- Figure 2.6: XRD pattern for GIS type materials
- Figure 2.7: Zeolite crystallization; a proposed mechanism by Burkett and Davis
- Figure 2.8: Zeolite crystallization; a proposed mechanism by Kirschhock et al.
- Figure 2.9: Ion-exchange sites on zeolite
- Figure 2.10: Brønsted acidic sites on the zeolite surface
- Figure 2.11: Lewis acid site formation on zeolite
- Figure 3.1: Zeolite synthesis steps
- Figure 3.2: synthesis steps for P type Zeolite
- Figure 3.2: Synthesis steps for DAC-Na Zeolite
- Figure 4.1: XRD machine working principle
- Figure 4.2: XRD results for NaP1 zeolite
- Figure 4.3: XRD results for DAC-Na zeolite
- Figure 4.4: SEM analysis for NaP1
- Figure 4.5: SEM analysis for DAC-Na
- Figure 4.6: AFM result for NaP1 (2-dimensional)
- Figure 4.7: AFM result for NaP1 (3-dimensional)
- Figure 4.8: AFM Analysis: Particle size distribution for NaP1 zeolite
- Figure 4.9: AFM result for DAC-Na (2-dimensional)
- Figure 4.10: AFM result for DAC-Na (3-dimensional)
- Figure 4.11: AFM Analysis: Particle size distribution for DAC-Na zeolite
- Figure 4.12: FT-IR result for NaP1 (A5) transmission mode
- Figure 5.1: Thermogravimetric study of LDPE pyrolysis with NaP1
- Figure 5.2: Thermogravimetric study of LDPE pyrolysis with DAC-Na

Chapter 1: Introduction

1.1 Background

Recently, Pakistan is suffering from an energy crisis. Current energy shortfall^[1] is 5,800 MW which is expected to increase with years. To take over the crisis, the nation of Pakistan is seriously indulged in research. They are working hard to develop new, cheap, and sustainable methods of energy generation, as well as trying to minimize energy consumption in the industrial sector.

The project “synthesis and characterization of catalysts used for petrochemical industry” is all about developing improved catalysts for minimizing energy consumption in various petrochemical reactions with cost and environmental effective protocol. Figure 1.1 depicts less energy consumption with catalysis is achieved for same chemical reaction.

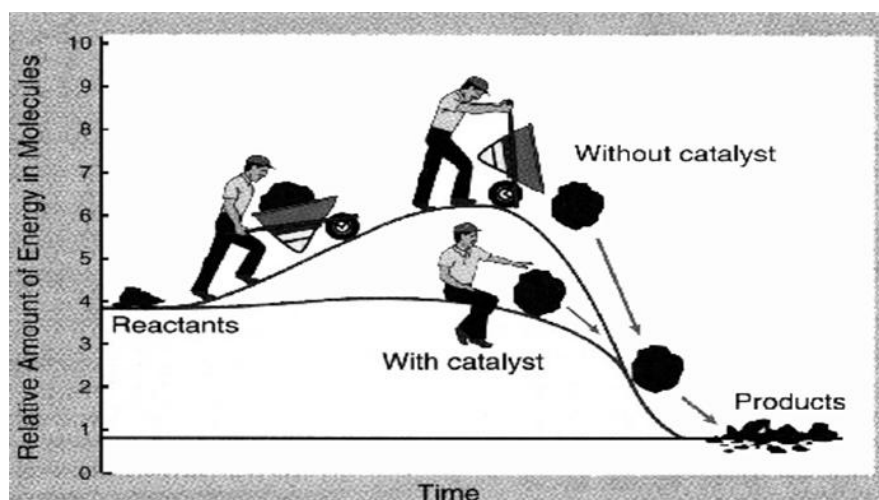


Figure 1.1: Comparison of chemical reaction with and without catalyst.

Catalysts are chemicals that are used to accelerate chemical reactions. The reactions are accomplished in less time and at lower operational conditions (temperature, pressure etc).

Energy minimization seems to be unimportant on laboratory scale experiments, but when we need to process a certain product at the industrial scale, catalyst utilization becomes mandatory. More importantly, it does not only reduce the energy required to accomplish a certain reaction, but also causes improvement of product quality. Catalysts put a positive effect on the environment because less waste is produced during the catalytic process. Figure 1.2 describes various impacts of catalysis in the process industry involving energy minimization, new processes development, new products synthesis, and utilization of novel feed stock for a reaction, lesser production cost, and development of environment friendly processes.

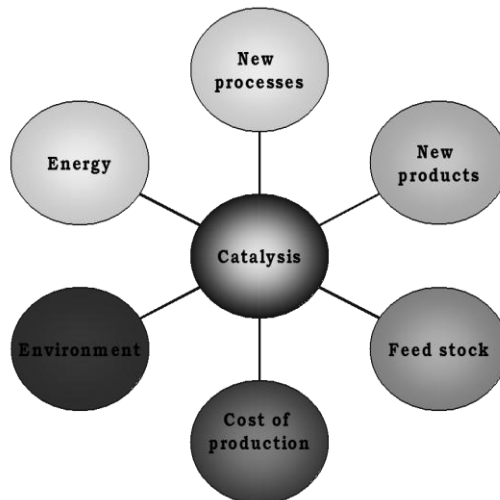


Figure 1.2: Impact of catalysis in Process Industry

1.2 An Introduction to Petrochemical Industry

The petrochemical industry is a distinctive branch of the chemical industry that deals with chemicals derived from crude oil.^[2] 90-95% of Crude Oil when refined is used as an energy source, and the remaining is converted into feedstock for the petrochemical industry. Table 1.1 describes origin of the petrochemical industry and various examples of petrochemicals.

Petrochemicals- The origin
Crude oil ↓
Refinery ↓
Feedstocks Gas, Naphtha, Gas Oil, Kerosene ↓
Chemical industry ↓
Basic chemicals Ethylene, Propylene, 1.3-Butadiene ↓
Petrochemical industry ↓
Petrochemicals PE, PP, PVC, PS, etc.

The chemical industry is a wide range industry, dealing with agricultural chemicals, pharmaceuticals, paints, food items, explosives, industrial gases and others. Figure 1.3 describes a chart showing various sub divisions of products of the chemical industry, where coatings (5%),

adhesives & sealants (1%), polymers, synthetic rubber & fibers (14%) and Bulk petrochemicals & organics (17%) are showing the role of petrochemicals in all chemical industries. 37% of chemical industry is the part of the petrochemical industry.

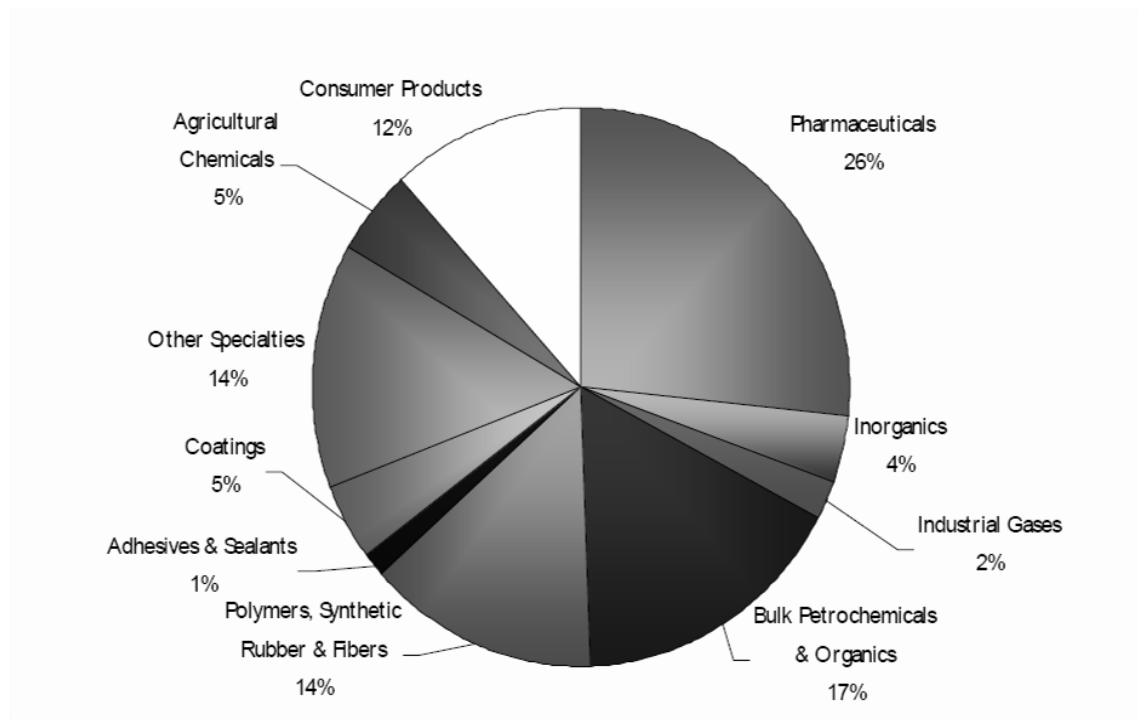


Figure 1.3: Chemical Industry products

Various kind of chemical reactions involved in the petrochemical industry are called “petrochemical reactions”. Some of the major petrochemical processes are:

- Cracking
- Reforming
- Polymerization
- Alkylation
- Isomerization
- Sweetening process

These processes can be accomplished by two famous routes:

- Thermal
- Catalytic

By applying high temperature conditions at an industrial scale means a huge amount of power consumption. Usually thermal reactions are accomplished at the temperature range of 400°C to 1000°C. This higher energy consumption has risk of uncontrollable heat. If temperature maintenance system fails, risk of plant explosion is always there.

Meanwhile, use of catalysts to accelerate the rate of reactions involved in the petrochemical industry is highly appreciated. Though purchase cost of catalyst is significantly high at present, efficient regeneration of catalysts in the end of reactions make it acceptable to be used. Because

it requires low temperature and moderate pressure conditions for reactions to be taken place with high rate.

1.3 History of Catalysis in the Petrochemical Industry

If we go through the history of catalysis in the petrochemical industry, we see three generations of catalysts.

a) Generation-1

Initially, petrochemical reactions were accelerated by using liquid acids (HF, sulphuric acid etc). They were cheap, easily available, and effective. But they had to be abandoned for three important reasons;

1. Acids are corrosive, their utilization simply decrease the life of catalytic reactors.
2. As they are liquids, process operators could not control their activity during the reaction.
3. They are dangerous in handling, as well as they create serious environmental problem when accumulated in waste.

b) Generation-2

After extensive research, scientists were able to replace liquid acids with solid catalysts having pH in acid range, for example silica. This development was advantageous in several aspects. One was being solid, they were easy to handle. They had no such environmental issue. Neither have they caused noticeable corrosion. Moreover, reaction control was accomplished easily by simply customizing the acidic level of solids by mixing basic solids in it. For example, to control the pH of silica, a certain amount of alumina was mixed, and hence a catalyst for a specific reaction was prepared. In some reactions, just a layer of suitable metal was sufficient for reaction acceleration. The Generation-2 was much better than Generation-1. The only problem was shorter life of the catalyst, rapid deactivation was observed. The reason was deposition of carbon on the catalyst surface, and regeneration was difficult to achieve. But the research never ends. Hence catalysts in petrochemical industry shifted into new era.

c) Generation-3

Since the solid acids used previously were amorphous in nature. scientists were able to synthesize new crystalline solids having the basic building block of silica. In other words, Zeolites (crystalline aluminosilicates) were started to be synthesized. Due to crystalline nature of this generation's catalysts, they were more efficient and long life catalysts (even years).

d) Modern catalyst

Modern catalyst being used in the petrochemical industry is the continuation of Generation-3. They are metal-loaded crystalline aluminosilicates having very small crystal size (nano level). The concept of nano crystal is “smaller the crystal size, more surface area is exposed to reaction”, hence the catalyst becomes more efficient. All the present research in the field of catalysis moves around a single objective: To improve zeolitic crystallization conditions for the sake of improved crystallinity and smaller size.

Chapter-2: Literature review

2.1 Introduction

Zeolites are crystalline solids made of silicon, aluminum, and oxygen that form a 3-D framework with cavities and channels inside where cations, water molecules, and/or other small molecules may reside.^[3] Zeolites were introduced in 1954, for the very first time, as adsorbent in industry for separations and purifications.^[4] Now their main use is in petrochemical catalysis. Because of their unique porous properties, zeolites are now used in a variety of applications with world production estimated to be in the range of 2.5 million to 3 million metric tons (Mt) in the year 2008.^[5]

Zeolites are of many forms, geometrical shapes, compositions and porosity. But they can be classified into three categories with respect to silica-alumina ratio.

1. Low silica-alumina ratio Zeolites
2. Moderate silica-alumina ratio Zeolites
3. High silica-alumina ratio Zeolites

Silica-alumina ratio plays an important role when we are going to select a catalyst for a reaction. Silica is an acidic solid. On the other hand, alumina is a basic solid. So on combination, their proportion does affect the acidity level of crystal. And acidity of crystal dictates its merit as a catalyst for a certain reaction.

2.2 Crystalline Microporous Materials: Zeolites

According to the classification made by IUPAC (International Union of Pure and Applied chemistry), porous solids can be grouped into three categories, depending on their pore diameter:

1. Microporous materials (whose porous diameter is less than 2 nm)
2. Mesoporous materials (whose porous diameter is greater than 2 nm and less than 50 nm)
3. Macroporous (whose porous diameter is greater than 50 nm)

Zeolites have unique character. Initially, during crystallization, they form microporous crystals, but soon these small crystals combine and form mesoporous aggregates.^[6]

2.3 Discovery and Applications

Discovery of natural zeolites is claimed to have happened in 1756 by almost all zeolite researchers. 38 different types of natural zeolites are found all around the world.^[7] Their application is limited to absorption, and cannot be used for today's advanced catalysis; The reason is impurity as well as low crystallinity (obviously due to impurities). For catalysis, synthetic zeolites of controlled crystallinity, morphology, and quality are used. Scientists used to synthesize very unique type of frameworks of different zeolites, and 190 different kind of synthetic zeolites are identified for various applications including absorption, molecular sieving, ion-exchange processes, and catalysis.

The most unique application of zeolites is hydrogen storage within its framework.^[3,6] Zeolites are also being merged in the biomedical area of science, because nano crystals of Zeolites are excellent drug carriers, and this application is limited to few zeolites and is subject to toxicity level. Zeolite is the most diverse field of study since 1950s and with the passage of time, more and more interest has been developed. Application of zeolites has expanded to wide horizon. Table 2.1 is created to state expanded number of publications on zeolite since its discovery.

Year	Known Structure types	Filed U.S. patents	Commercialized structure types
1960-1969	27	2900	3
1970-1979	11	4900	1
1980-1989	26	7400	2
1990+	61	8200	5
Total	125	23400	11

Table 2.1: Zeolite topic of research for decades^[8]

2.4 Zeolite Structure

Zeolites are tecto aluminosilicates with a formal composition $M^{n+}_2/nO \cdot Al_2O_3 \cdot xSiO_2 \cdot yH_2O$ (n = valence state of the mobile cation, M^{n+} and $x \geq 2$), in that they are composed of TO₄ tetrahedra (T = tetrahedral atom, i.e., Si, Al), each oxygen atom is shared between adjacent tetrahedra, which leads to the framework ratio of O/T being equal to 2 for all Zeolites^[9]. A dimensional framework is formed by 4-corner connecting TO₄ tetrahedra. When a zeolite is made of pure silica without any defects, each oxygen atom at the corner is shared by two SiO₄ tetrahedra and charge is balanced. Figure 2.1 depicts zeolite structure building from single tetrahedra.

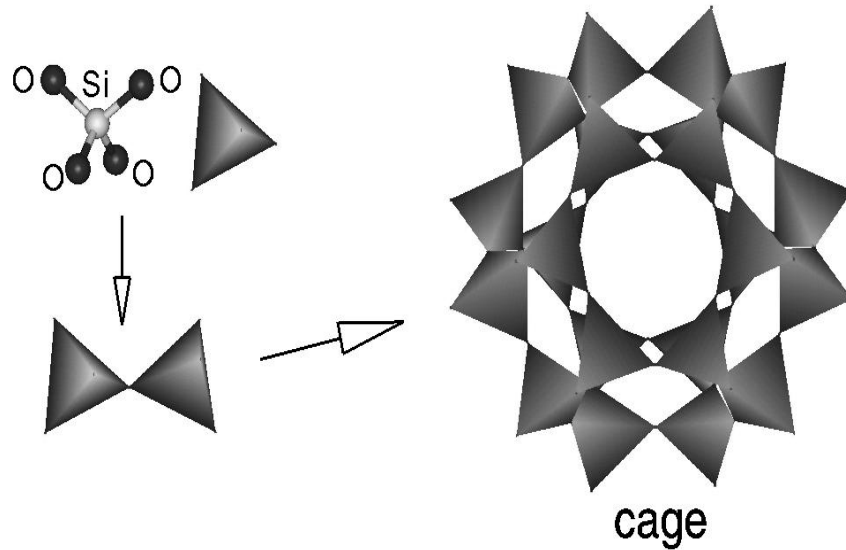


Figure 2.1: Zeolitic structure buildup

When silicon is replaced by aluminum, alkali metal ions, such as K^+ , Na^+ , alkaline earth ions, such as Ba^{2+} , Ca^{2+} , and protons, H^+ are typically introduced to balance the charges. Such formed framework is relatively open and characterized by the presence of channels and cavities. The size of the pores and the dimensionality of the channel system are determined by arrangement of TO_4 tetrahedra. More specifically, the pore sizes are determined by the size of the rings that are formed by connecting various numbers of TO_4 tetrahedra or T atoms. An 8-ring is designated to a ring comprised of eight TO_4 tetrahedra and is considered to be a small pore opening (0.41 nm in diameter), for example a framework of silicon and beryllium of T-atom arrangement will form such 8-membered ring (Figure 2.2)

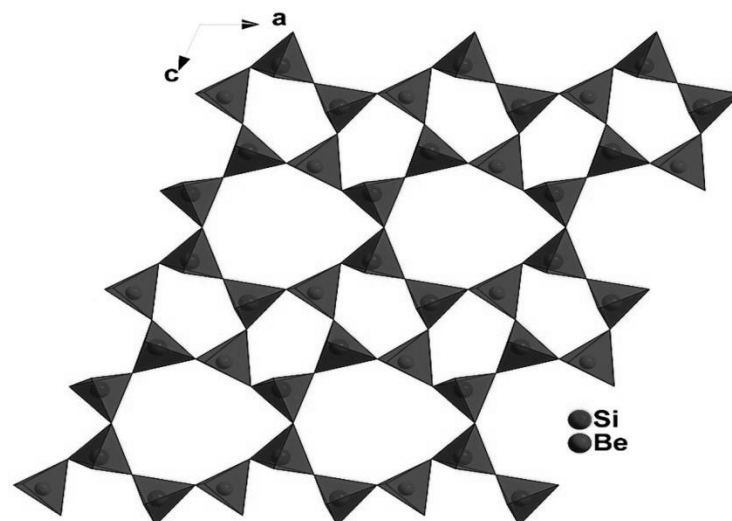


Figure 2.2: A schematic 8 membered zeolitic ring

A 10-ring is a medium one (0.55 nm), and a 12-ring is a large one (0.74 nm), when rings are free of distortion. Depending on the arrangement or the connection of various rings, different structures or pore openings, such as cages, channels, chains, and sheets, can be formed. Figure

2.3 shows some of these subunits, in which each cross point is designated to TO_4 tetrahedra for clarity.

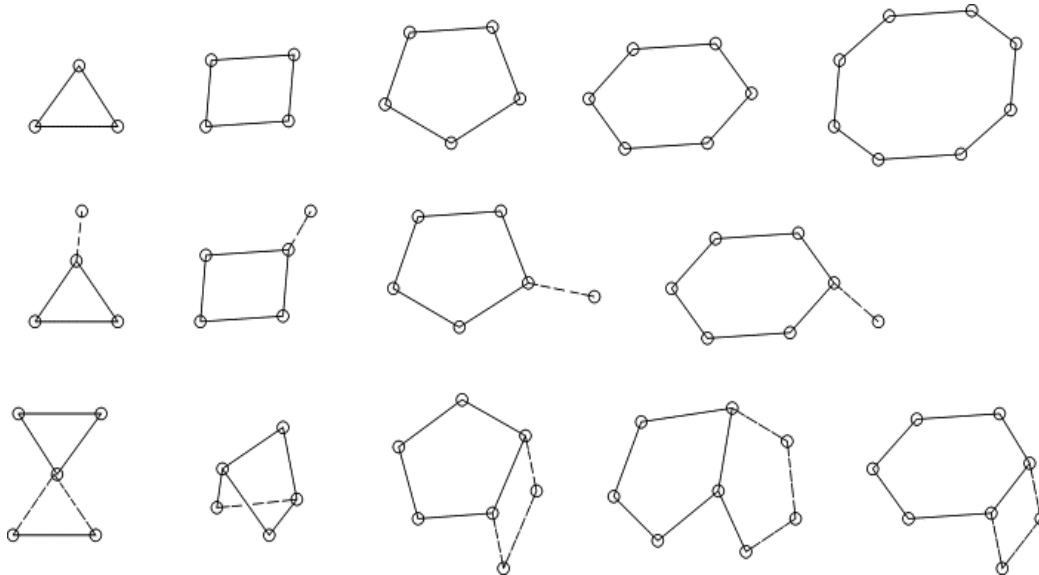


Figure 2.3: subunits of zeolite structure

A nomenclature similar to that used for cages has also been developed to describe channels, chains, and sheets. Different frameworks are formed by stacking various subunits and/or with different stacking sequences. There are 133 confirmed zeolite framework types. Figure 2.4 shows DAC type Dachiardite Zeolites' framework^[10], indicating five heptagonal rings are attached to each other by six pentagonal rings, when viewed along [001].

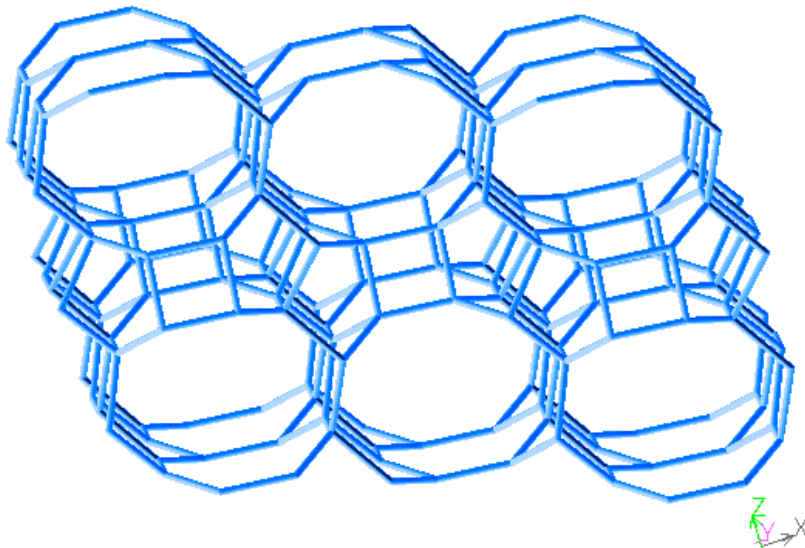
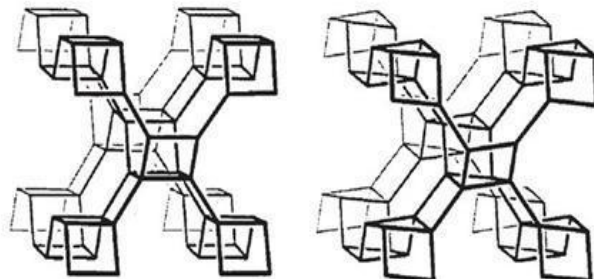


Figure 2.4: DAC type Dachiardite Zeolites' framework

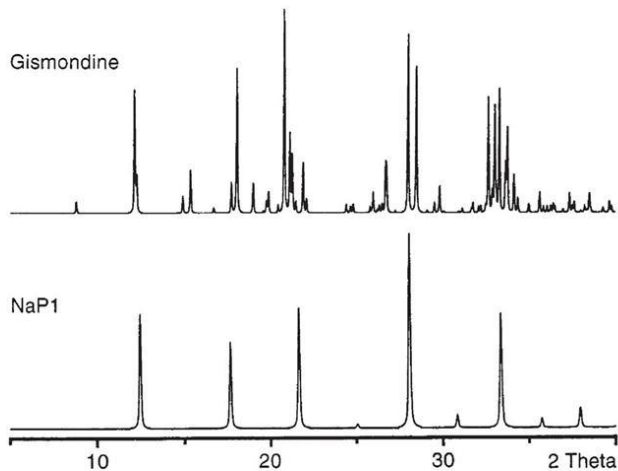
All members in a zeolite family are isotypic but differ considerably in their conformation. A useful example is GIS type zeolites, where Na-P1 and NaP2 is compared in Figure 2.5^[11], clearly showing both are isotypic but have different conformation.



Conformations of GIS-type materials. *Left: gismondine (P_{2,1}/c), right: NaP1 (I $\bar{4}$)*

Figure 2.5: GIS type materials conformation

The difference in these two conformations can clearly be seen in their XRD patterns (Figure 2.6)^[11]:



XRD powder patterns of two GIS-type materials (*top: gismondine, bottom: NaP1*)

Figure 2.6: XRD pattern for GIS type materials

2.5. Synthesis of Zeolites

Zeolites are normally prepared by hydrothermal synthesis techniques.^[12] A typical synthesis procedure involves the use of water, a silica source, an alumina source, a mineralizing agent, and a structure-directing agent. The sources of silica are numerous and include colloidal silica, fumed silica, precipitated silica, and silicon alkoxides. Typical alumina sources include sodium

aluminate, boehmite, aluminum hydroxide, aluminum nitrate, and alumina. The typical mineralizing agent is hydroxyl ion, OH⁻, and fluoride ion, F⁻. The structure-directing agent is soluble organic species, such as quaternary ammonium ion, which assists in the formation of the silica framework and ultimately resides within the intracrystalline voids. Alkali metal ions can also play a structure-directing role in the crystallization process.

The syntheses can be sensitive to the reagent type, the order of addition, the degree of mixing, the crystallization temperature and time, and the composition. There are numerous complex chemical reactions and organic-inorganic interactions occurring during the synthesis process. Depending on the mixture composition, the extent of reactions, and the synthesis temperature, at least four types of liquids can be yielded^[30]:

- (1) Clear solution that consists of molecular, monomeric, and ionic species only.
- (2) Sol or colloidal consisting of amorphous clusters with open structure (also called dispersed low density gel).
- (3) Sol or colloidal with dispersed amorphous clusters with dense structure (also referred to as separated high density gel).
- (4) Sol or colloidal with metastable crystalline solid nanoparticles (also called solid phase).

Zeolites are subsequently formed through nucleation and crystallization from these systems. Various studies have been carried out to establish understanding on the crystal growth mechanisms on molecular level and the crystal-building units.

2.5.1 Synthesis Mechanism

At least three types of crystal building units have been suggested for the growth of Zeolites:

1. Tetrahedral monomeric species are considered as the primary building units
2. Secondary building units are the crystal building units
3. Clathrates are the building units in the nucleation and crystallization of Zeolites.

Two recent synthesis models are outlined below.

Figure 2.7 illustrates the mechanism of structure direction and crystal growth in the synthesis of TPA-Si-ZSM-5 proposed by Burkett and Davis^[13]:

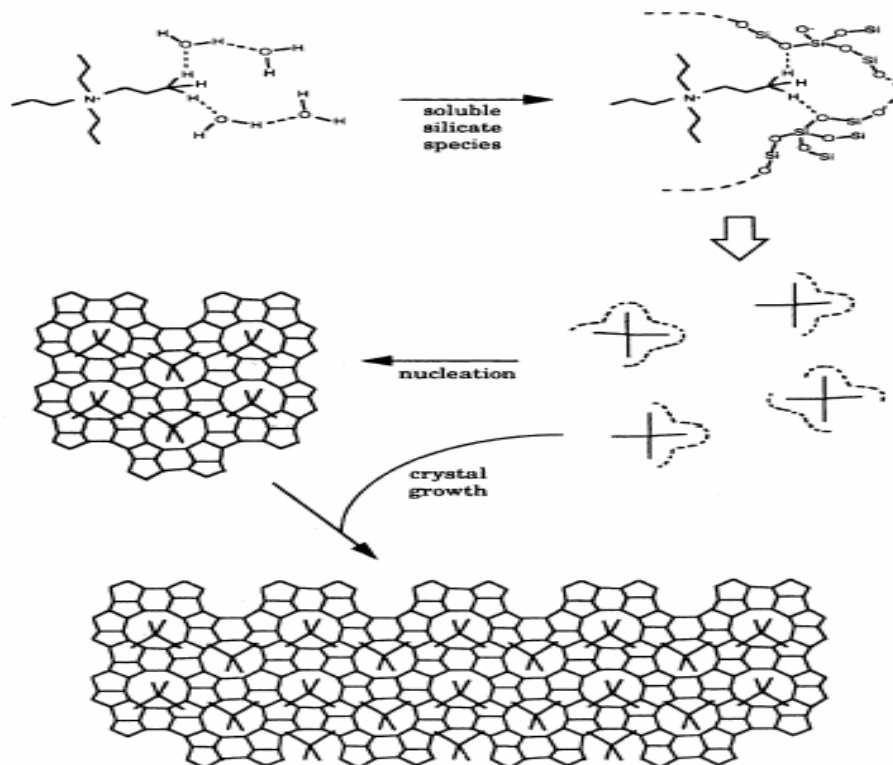


Figure 2.7: Zeolite crystallization; a proposed mechanism by Burkett and Davis

During the synthesis, the inorganic-organic composite clusters are first formed by overlapping the hydrophobic hydration spheres of the inorganic and organic components and subsequent releasing of ordered water to establish favorable van der Waals interactions. Such inorganic-organic composite clusters serve as growth species for both initial nucleation and subsequent growth of zeolite crystals. The nucleation occurs through epitaxial aggregation of these composite clusters, whereas the crystal growth proceeds through diffusion of the same species to the growing surface to give a layer-by-layer growth mechanism.

Another mechanism, called “nanoslab” hypothesis^[14], builds on the mechanism discussed above. The difference is that the inorganic-organic composite clusters form “nanoslab” through epitaxial aggregation first. Such formed “nanoslabs” aggregates with other “nanoslabs” to form bigger slabs as shown in Figure 2.8:

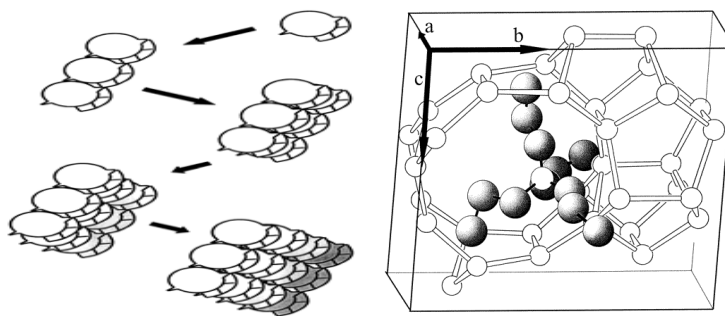


Figure 2.8: Zeolite crystallization; a proposed mechanism by Kirschhock et al.

2.5.2 Effects of Structure-Directing Agent

When different organic molecules as structure-directing agents are included in otherwise an identical synthesis mixture, zeolites with completely different crystal structures can be formed. For example, when N,N,N-trimethyl 1- adamantammonium hydroxide is used as a structure-directing agent, zeolite SSZ-24 was formed, while ZSM-5 was produced by using tetrapropylammonium hydroxide as structure-directing agent. In addition, the choice of a structure-directing agent can affect the synthesis rate.^[15] The geometry of the structure-directing agent has a direct impact on the geometry of the zeolite synthesized. For example, SSZ-26 is a zeolite with intersecting 10- and 12-ring pores, and was synthesized with a prior design using a propellane-based structure-directing agent.^[16] It has been demonstrated experimentally and through molecular force field calculations that the geometry of the pore sections of SSZ-26 matches very well with that of the organic structure-directing molecules and one structure-directing molecule is present in each channel intersection.^[17] ZSM-18 is an aluminosilicate zeolite containing 3-member rings and was synthesized using structure-directing agent, designed using molecular modeling.^[18] An excellent fit exists between the zeolite cage and the organic structure-directing agent.

2.5.3 Effects of Heteroatoms

The addition of small quantities of tetrahedral cations, such as Al, Zn, B etc, to the synthesis mixtures has dramatic effects and results in significantly different zeolite structures when using identical structure-directing agents. Table 2.2 compared some systems.

Organic agent	SiO ₂	SiO ₂ /Al ₂ O ₃ <50	SiO ₂ /B ₂ O ₃ <30	SiO ₂ /ZnO <100
C8H20N	ZSM-12	Zeolite Beta	Zeolite Beta	VPI-8
C16H32N4	ZSM-12	Zeolite Beta	Zeolite Beta	VPI-8
C13H24N*	ZSM-12	Mordenite	Zeolite Beta	Layered Mater.
C13H24N*	SSZ-24	SSZ-25	SSZ-33	--
C13H24N*	SSZ-31	Mordenite	SSZ-33	VPI-8

Table 2.2: Effect of heteroatoms for Zeolite synthesis

* With different molecular structures

For example, when other synthesis parameters are kept the same with tetraethylammonium cation, TEA⁺, as a structure-directing agent, ZSM-12 is formed when the ratio of SiO₂ and Al₂O₃ is greater than 50. When a small amount of alumina is added, zeolite beta is formed. Further addition of alumina to reach a ratio of 15 of SiO₂/Al₂O₃, ZSM-20 is then synthesized. The substitution of divalent and trivalent tetrahedral cations for Si⁴⁺ in the synthesis mixtures results in a negatively charged zeolite framework, which will coordinate more strongly with both the organic structure-directing cations and the inorganic cations, such as alkali metal cations. In addition, the change of both the cation-oxygen bond lengths and the cation-oxygen-cation bond angles would have appreciable influences on the formation of building units.^[19]

2.5.4 Effects of Alkali Metal Cations

The presence of alkali metal cations is required for the vast majority of zeolite syntheses at basic conditions. A small concentration of alkali metal cations in aqueous solutions significantly increases the dissolution rate of quartz, up to 15 times as much as the rate in deionized water.^[20] It is generally accepted that the presence of alkali metal cations can accelerate the rate of nucleation and crystal growth of high-silica zeolites. However, it was also found that too much alkali metal cations may result in competition with the organic structure-directing agent for interactions with silica such that layer-structured products can result.

2.5.5 Ageing and Seeding

Once the gel is made, it can either be heated straight away, or left to age at room temperature prior to use. The ageing process is said to provide a period for nuclei to form, which are the building blocks of the final crystals. Traditionally nucleation takes place in the initial heat up period of the gel to reaction temperature. However, if microwave heating is employed, the slow heat up phase is effectively eliminated, and the ageing step is beneficial. If the precursor nuclei are present already then the crystallization stage can occur sooner and reduce the heating time. As an alternative to ageing, seed crystals, or even 10% by weight of aged gel, can be added to the zeolite gel.^[21] After adding the aged gel or seed crystals, the rate of crystallization was found to be enhanced compared to unaged zeolite gels.

2.5.6 Stirring

Stirring during the ageing process or reaction can cause an increase in collisions between species in solution, and prevents a local depletion of reagents around the forming crystals. In some instances this may be beneficial and lead to a reduction in reaction time, through increased rates of nucleation. However, stirring may also break down existing species and stimulate production of undesired structures. For example, in the synthesis of zeolite Na-X (FAU), Freund performed the same reaction with differing stirring speeds ranging from 0 to 350 rpm.^[22] Whilst the time taken to yield crystalline products decreases with increasing stirring speed, the purity is compromised by the co-crystallization of zeolite Na-P1 (GIS).

2.5.7 Nucleation and Crystal Growth

Barrer^[23] described the processes involved in crystallization of a zeolitic product. Firstly, small aggregates form unstable nuclei, some of which grow large enough to become stable nuclei, whilst the others dissolve. Material in the solution is deposited on the stable nuclei, and these form crystallites. This process is relatively slow, as the crystals form by a condensation polymerization.^[23]

2.5.8 Heating Conditions

The heating conditions for the precursor gel tend to mimic those which form zeolites in nature. Naturally occurring zeolites are often found in lava flows or volcanic sediments, and so temperatures over 200°C and high pressures (> 100 bar) were typically used in early syntheses.

With the use of reactive alkali-metal aluminosilicate gels, however, lower temperatures and pressures can be used enabling synthesis to take place at around 100°C and under autogenous pressure. Ostwald's Law^[24] of successive transformation is very important in the consideration of zeolite synthesis. Thermodynamically the least stable, and is replaced by ever more stable phases until the most stable product is formed. Products may persist if there is a significant activation energy barrier to the more stable phase.^[24] All zeolite structures are metastable with respect to more dense phases. Due to these transformations, if a relatively unstable product is desired, it is essential to stop reaction at the appropriate time and to isolate the product by filtration. This removes the structure from the reaction medium, and therefore it can no longer be broken down and further transformed as solid-state rearrangements have a prohibitively large energy barrier^[25].

Finally, there is the choice of whether to heat the gel in a microwave oven or in a conventional oven.

2.6 Zeolitic Catalysis Mechanism

In all silica zeolites, the overall charge of the surface is zero, and the formula unit of the material is SiO₂. Introduction of aluminum or another element with valence less than 4 creates a deficiency of positive charge, which needs to be compensated. In high silica zeolites, where the amount of negatively charged surface sites is low, the positive charge on the organic structure directing agent can act as a counter ion. However, the structure directing agent molecules are typically bulky and as the amount of negatively charged sites increases, inorganic cations of alkali metals need to be added to the reaction mixture in order to compensate the excess of negative charge on the surface. This way ion-exchange sites are created on the surface of the zeolite and can be exchanged by a variety of different cations to modify the zeolite properties.^[26,27] As shown (Figure 2.9):

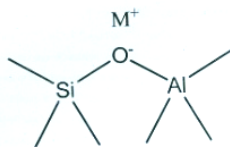


Figure 2.9: Ion-exchange sites on zeolite

Replacing an alkali cation by a proton is one of the important modifications from the practical standpoint, as it creates Brønsted acidic sites on the zeolite surface (Figure 2.10):

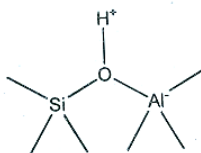


Figure 2.10: Brønsted acidic sites on the zeolite surface

The degree of acidity depends on the zeolite framework and proximity to other acid sites. Thermal dehydration of zeolites results in release of water and creation of Lewis acid site (Figure 2.11):

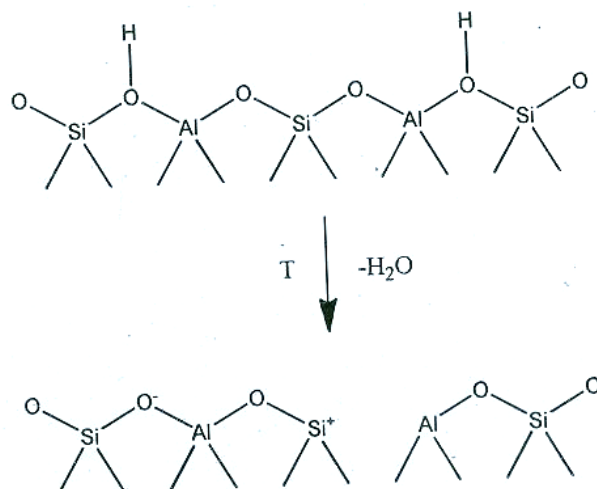


Figure 2.11: Lewis acid site formation on zeolite

Acid sites on the zeolite surface exhibit catalytic activity towards a large number of reactions. One of the first catalytic applications of zeolites was in the petrochemical industry, where faujasite zeolite replaced amorphous aluminosilicates in the fluid catalytic cracking (FCC) process.^[28] Many more types of zeolite have found catalytic application for hydrocracking, hydroisomerization, catalytic dewaxing, and other reactions. The combination of acid site strength with the pore size and profile offer unique environment around the acid sites that can be tuned for specific catalytic applications. The petrochemical industry is not the only one using zeolite-based catalysts. Zeolites are being used in the automotive industry in catalytic converter systems for decreasing emission levels of nitrogen oxides (NO_x). In a typical three-way catalytic converter metal-exchanged zeolite catalyzed reduction of NO_x into nitrogen by using hydrocarbons present in the exhaust fumes as a reducing agent.^[29] Finally, zeolite catalysts are evaluated in the pharmaceutical industry for fine chemical synthesis.^[30]

2.7 Nanostructured Zeolites

The interest in decreasing the zeolite crystal size for applications in catalysis and adsorption lies in microporosity of zeolites. The size of micropores in zeolites does not exceed 15 angstroms, and for the majority of zeolite frameworks is around 5-6 angstroms in diameter. The small pore size poses diffusion limitations in the case of large crystals. Decreasing the crystal size not only shortens the diffusion path lengths but also increases the fraction of the external surface area relative to the total surface area of the zeolite.^[31] Active sites located on the external surface are substantially easier to access than the active sites inside the zeolite pore network. The number of synthesized nanoscale zeolite structures is limited to LTL, LTA, FAU, GIS, DAC and MOR.

Nanoscale MFI (ZSM-5, Silicalite-1), BEA and FAU zeolites have been studied the most widely due to a wide range of reaction conditions leading to the desired framework type.

2.8 Zeolite synthesis steps

Synthesis of P type zeolite and DAC type zeolite was accomplished in experimental part of this Work. The most common schematic diagram for operations involved in Zeolite synthesis is given (figure 3.1):



Figure 3.1: Zeolite synthesis steps

However duration and sequence of operations are adjusted accordingly with types of reactants involved. For example, Ando et al.^[32] depict manufacturing method of zeolite from waste, where silica source was exhaust gas treatment sludge from an optical fiber manufacturing plant and alumina source was common aluminum scrap. So definitely, mixing of these larger particles would require longer time as well as 100% mixing would need an extended operational cost. So two extra operations prior to mixing would be crushing and milling. Similarly, Sarah et al.^[33] used tetraethylorthosilicate (TEOS) as silica source and aluminum isoperoxide (AIP) as alumina source as well as tetramethyl ammonium hydroxide (TMAOH) as structure directing agent, as a result, removal of organic content after crystallization needed centrifugation and removal of carbon attached within zeolite framework required calcinations in the end, hence two additional operations were performed to produce NaY type zeolite. Clearly, selection of reactants for zeolite synthesis affects the operational cost and it widely varies depending upon the purpose for which zeolite is being synthesized.

In our case, as have been discussed in earlier chapter, better zeolite catalyst means a product having crystal size of nanoscale. Meanwhile lesser time with lower operational conditions are also the part of our interest. To accomplish synthesis of products very close to our interest, two approaches were possible:

1. By introducing organic structure directing agent during mixing not only reduces crystallization time and crystal size but also controls the silica to alumina (SAR) ratio in the final product. But it also needs rotary evaporation prior to crystallization and centrifugation in post crystallization. Calcination of final dry product is also required.

2. Another approach is to use highly basic medium, this will give nanocrystalline zeolite but final SAR will be very low, so acid leaching to remove extra aluminum from zeolite framework is done in the end. This process is called dealuminization. Elodie et al.^[34] showed that nitric acid leaching from NaY can improve silica to alumina ratio without damaging framework.

Instead of going through single approach to synthesize P type zeolite and DAC type zeolite, we tried to synthesize P type zeolite in higher pH medium and DAC type zeolite in organic medium. In this way, we got a unique chance to apply both products in a single catalytic application, pyrolysis of polyethylene (described in part 4), and compare the results obtained.

2.9 Synthesis of Na-P1

Na-P1 zeolite also known as gobbinsite having chemical composition $\text{Na}_6(\text{H}_2\text{O})_{12}[\text{Si}_{10}\text{Al}_6\text{O}_{32}]$.^[35] GIS type gobbinsite zeolite has always been of wide interest due to high ion-exchangeable sites and several researchers worked on its Gel chemistry and framework structure^[36-39]. Barrer et al.^[40] suggested three phases of gobbinsite; cubical, orthorhombic and tetragonal. After few years, Baerlocher et al.^[41] suggested cubical phase as Na-P1 and they refined its chemistry by using a unit cell of pseudo-cubic pattern and space group I^4 . Then, in 1990 hensen and hiw coworkers suggested tetragonal phase as Na-P2^[42]. In 2001, Baerlocher^[43] suggested orthorhombic phase as melionoite MER zeolite while before that in 1985, Gottardi and coworker showed orthorhombic phase not the part of P-type zeolite family but has a great resemblance to zeolite K-M family^[44].

GIS type framework shows exceptional flexibility among both zeolite Na-P1 and Na-P2. So extra framework molecular ions, chemical composition and dehydration state may be the criteria of conformation^[45,46]. In 1993, Hansen and co-worker^[47] revealed valuable information about chemical composition and crystal structure. They characterized P-type zeolites in three categories, low silica (8 to 10 atoms of silicon in a cell) phase as P1, medium silica (10 to 12 atoms of silicon in a cell) phase as P2 and high silica (12 to 13 atoms of silicon in a cell) phase as tetragonal silica. However, this classification did not satisfy eight types of P zeolite suggested previously by W.C. Beard.^[48] So, symmetry of low silica Na-P zeolite suggested by Alberti et al.^[49] was always been the part of discussion in literature. Synthesis parameters like reactants type and quality, crystallization temperature and duration for Na-P1 is another issue of discussion. Many researchers utilized fly ash coal to synthesize Na-P1 and discussed synthesis parameters. For example, Detkowski et al.^[50] synthesized various zeolitic phases including Na-P1 from fly coal ash by crystallization at 150°C for 12–48 hours. Dusica et al.^[51] discussed effect of silica to alumina ratio of Na-P1 and utilized coal fly ash during its synthesis. Mouhtaros et al.^[52] discussed synthesis of GIS type zeolite with 10-15% yield from sulphocalcis fly ash. Querol et al.^[53] synthesized various phases including 40-55% Na-P1 zeolite from narcea fly ash.

Adamczyk and co-worker^[54] reported joint phase formation of Na-P1 and analcime from polish fly ash and discussed the phase shift from Na-P1 to analcime with rise of temperature. Hence a number of publications explaining various methods of producing Na-P1 type zeolite from fly ash. These are very good examples of utilization of fly ash generating from coal power plants to synthesize zeolite. But still the major utilization of coal fly ash is the cement industry as well as treatment of waste effluent.^[55] Synthesis of Na-P1 from fly ash cannot be utilized to observe various valuable industrial applications because this process does not produce pure, single phase zeolite. Synthesizing Pure Na-P1 zeolite without any extra framework ion provides scope in various applications, because it contains high sodium and aluminum contents within its framework. This creates lot of ion-exchange sites and absorbance capacity within zeolite crystals making it abundantly utilized in mass separation applications^[56] (e.g. heavy metal absorption) and catalysis.^[57] Adams et al.^[58]

suggested P type zeolite as a low temperature calcium binder for various applications. Abraham Araya^[59] claimed P type zeolite production from metakaolin and its utilization as in detergent composition. Dong and co-worker^[60] established P-type zeolitic membrane on alumina support for mass transportation applications. Catalytic application of Na-P1 type zeolite is not as reported as its utilization as gas-separator and absorber in industry. However many reactive metals can be either absorbed inside Na-P1 pores or be exchanged with sodium cation present in extent in zeolitic framework. Jeong et al.^[61] utilized Na-P1 for LDPE pyrolysis and compared the results with those obtained from catalytic pyrolysis of LDPE when utilizing HY type zeolite. So, new area of research can be the catalytic application of Na-P1 type zeolite in hydrocarbon industry.

2.10 Synthesis of DAC-Na

Dachiardite-Na, $[(Na_4(H_2O)_{13})[Al_4Si_{20}O_{48}]]$ was described and named by D'Achiardi in 1906^[63]. while DAC series was elevated by Coombs et al.^[62] who included two types of DAC zeolites DAC-Na and DAC-Ca having two different cations as extra framework part zeolite. both of these zeolites have monoclinic crystalline structure^[63] and have very close geometry to Ferrite type zeolite. Natural occurrence of Dachiardite is mostly abundant for DAC-Ca while DAC-Na was found in a single miarolitic cavity in the silicon carbonatite sill.^[64] Natural Dachiardite-Na type zeolite has very high crystallinity level but also found in extremely impure form. Refining of natural zeolites are performed by hydrothermal recrystallization, that makes zeolite more costly because now mining cost is also included along with purification cost. That is why; pure zeolites are synthesized through hydrothermal crystallization. Dachiardite type zeolites are very popular choice for catalysis in petrochemical industries for catalytic cracking processes. Hayim Abrevaya et al.^[65] claimed catalytic cracking of naphtha by using a combination of various zeolites including Dachiardite type zeolite. Conversion of ketones over metal containing Dachiardite type catalysts was suggested by Tracy J. Huang et al^[66].

2.11 Characterization

Literally, characterization of a synthesized product means to classify where does the prepared product lies in the list of already prepared products with respect to quality, purity and reliability. To know this, various analytical techniques are used. In the present work, zeolites catalysts were characterized by using various analytical techniques such as X-Ray Diffraction (XRD), Scanning Electron Microscope (SEM), Scanning Probe Microscope (AFM) and Fourier Transform Infrared (FT-IR) analysis. Thermal behavior of both catalysts was characterized through Thermogravimetric and Differential Thermal Analysis (TGA/DTA).

2.11.1 XRD Analysis

X-ray diffraction is a nondestructive analytical technique that is used to determine crystalline structure of sample.^[67] Moreover crystal size can also be determined from XRD analysis, by using scherrer equation, that dictates that as the crystal size decreases, the reflections in the XRD pattern will be broadened:

$$\tau = \frac{K\lambda}{\beta \cos \theta}$$

Where K is the shape factor (K=0.94 for unknown shaped particles), λ is the X-Ray wavelength (1.5418Å in the case of Cu Ka radiation), β is the line width at half the maximum (FWHM), and θ is the Bragg angle.

In present work, instrument used to characterize the crystalline structure of sample materials was “STOE Theta/theta diffractometer”, having secondary monochromator, scintillation counter detector and cu source x-rays of wavelength 1.540598 Å. Finely grinded, powder sample was placed in aluminum plate of volume 0.30 cm³. Once scan was completed, digital peaks indication was performed by using X’pert Highscore software and then peak searching analysis were carried out with same software.

2.11.2 SEM Analysis

Scanning electron microscopy is the most popular, destructive characterization technique that provides information about surface topography, composition and microstructure of crystalline product. It is also used to determine the electrical conductivity of the sample.^[69] In our case, zeolites are non-conductors, so before conducting SEM analysis, a very thin layer of some conducting metal is coated over the sample to avoid scanning faults. In the present work, SEM analysis was done in JSM-64901-analytical scanning electron microscope. While conducting material coated was gold, it was sputtered by JFC-1500 ion sputtering device by using frequency 250Å.

2.11.3 AFM Analysis

Atomic Force Microscopy (AFM) is a destructive analysis used to determine the size of particles at nanoscale. This analytical technique uses a physical probe of very small diameter that scans

the sample. Image of the surface is obtained by mechanically selecting the scan area and moving the probe through selected surface, and probe-surface interaction is recorded as a function of position.

We have used JAFM-5200 scanning probe microscope for our analysis.

2.12 LDPE Pyrolysis

Low density polyethylene is a thermoplastic polymer derived from petroleum by “free radical polymerization” at high pressure, it was manufactured in 1933 for the first time by ICI (imperial chemical industry).^[82] Its main use has always been packaging. A survey, in 2009, stating annual worldwide market of polyethylene is 12.9 trillion Euro.^[83] LDPE is classified by the density range of 0.9 to 0.94 g/cm³. Due to its cheapest price, Polyethylene bags are widely used all around the world. In a result, LDPE disposal and waste management has become serious environmental problem. Due to its thermoplastic nature, it cannot be degraded at lower temperature, neither can be land filled. Another serious problem that always observed is its entrance in rivers. Indus Dolphin; worldwide famous, rare blind Dolphin resides in Indus River, Pakistan. A survey in 2001 stated the total population of Indus Dolphin as 602.^[84] In 2006, the population was 1600-1750 and in 2011, its population was counted as 802 in Dolphin Reserve (Guddo to Sakhar Barrage).^[85] The deaths of this beautiful specie is reported as “accidental trap in plastic bag”. In 2011, WWF (world wide fund for nature) organized an annual travelling nature cuvinial in F-9 park, Islamabad.^[86] Where two different themes “say no to plastic bags” and “Threats to Indus Dolphin” clearly stated the harmful environmental impacts of low density polyethylene in general and their dangerous impact to Indus Dolphins in particular. On the other hand, Industrial sector is clearly interested in manufacturing plastic bags, due to its bulk consumption. Somehow or other, used plastic bag’s open exposure can be minimized by waste management authorities. Waste recycling (re-polymerization) and thermal pyrolysis (depolymerization) are two common unit processes performed by city municipal. Another option could be the catalytic pyrolysis of LDPE. Many researchers have suggested different catalysts to perform catalytic pyrolysis. For example, Ali et al.^[87] utilized hydrocracking catalysts like NiMo loaded on [TiO₂+alpha alumina+AP-1+USY] extrudates, KC-2710 (AKZO Nobel), Z-713 (Zeolyst international), HC-100 (UOP) and RCD-8 (UOP) to evaluate the thermogravimetric study of catalytic pyrolysis of plastics. Lopez et al.^[88] used ZSM-5 zeolite as a catalyst to investigate the stepwise catalytic pyrolysis of various plastics. Sivakumari and coworker^[89] investigated the pyrolytic products of waste LDPE when using NiMo/Al₂O₃ as a catalyst. Tajeddin^[90] investigated thermal properties of polyethylene, stating degradation lies during 400-500°C. Lee et al.^[91] investigated catalytic pyrolysis of LDPE using spent FCC catalyst. Jeong et al.^[92] used amorphous silica–alumina catalysts (FSAs) to compare the thermal and catalytic pyrolysis of LDPE. In the present work, a comparative study of thermal and catalytic pyrolysis of LDPE by using two zeolite type catalysts is achieved by using Thermogravimetric analyzer.

The results show less temperature is required for catalytic pyrolysis of LDPE as well as lesser amount of wax as the residual constituents was observed.

Chapter 3: Experimental

3.1 Synthesis of Na-P1

Reactants we used, in this work were cheaper and easily available. Silica source was “Silica gel with humidity indicator (orange), having particles of 1-3 mm diameter (Schalau), and alumina source was sodium aluminate, anhydrous (Sigma-Aldrich), Base source was sodium hydroxide pellets (Uni-CHEM® chemical Reagents) and ultra pure water was used. These different sources were used in this molar ratio: $4\text{NaOH}:\text{NaAlO}_2:3\text{SiO}_2:55\text{H}_2\text{O}$

Process details

The main objective was to obtain nanocrystalline zeolite in reflux flask by mean of increased pH of the system. The stepwise description of each operation is described below:

1. Synthesis gel preparation

Base source: 80 ml ultra pure water H_2O was mixed with 0.723g NaOH, very gently until dissolved, to make 80ml of 0.225M NaOH solution. The pH of the solution was noted as 9.2. This solution was divided into two equal parts, 40ml each (almost).

Silica source: 15.16g NaOH was added in 20ml H_2O after which silica gel of weight 16.5g was added to it. It was heated at 50 °C for 20 minutes, under constant stirring (electric stirrer at 150rpm). A clear (pale orange) solution was obtained. Its pH was found to be 13.8. Then one half of solution obtained from step-a was added and gently mixed to it. New pH was 13.5.

Remaining half solution obtained from step-a was mixed with 8.258g NaAlO_2 . Again a clear solution was obtained, having pH 13.9.

d. The last step of synthesis gel preparation was addition of silicate solution into aluminate solution, quickly a thick, white gel was appeared. It was mixed at 200rpm with electric stirrer. Its pH was noted to be 13.

2. Nucleation

The gel was mixed under the same parameter for 48 hours. Constant stirring during nucleation did not allow gel specie to make crystallites of larger size.

3. Crystallization

After nucleation, the solution gel was shifted to round bottom flask and introduced into a total reflux setup. Solution was heated up to 100 ± 5 °C while constantly stirring at 200 rpm (this time it was done with magnetic stirrer). Crystallization time was different for different experiments; the process was repeated for six times to collect samples for crystallization time of 12, 14, 16, 18, 20 and 22 hours.

4. Washing

All samples were washed immediately, with cold ultra pure water until remaining pH was up to 9.

5. Drying

After washing, samples were introduced into air oven, and dried at 100 °C for 12 hours.

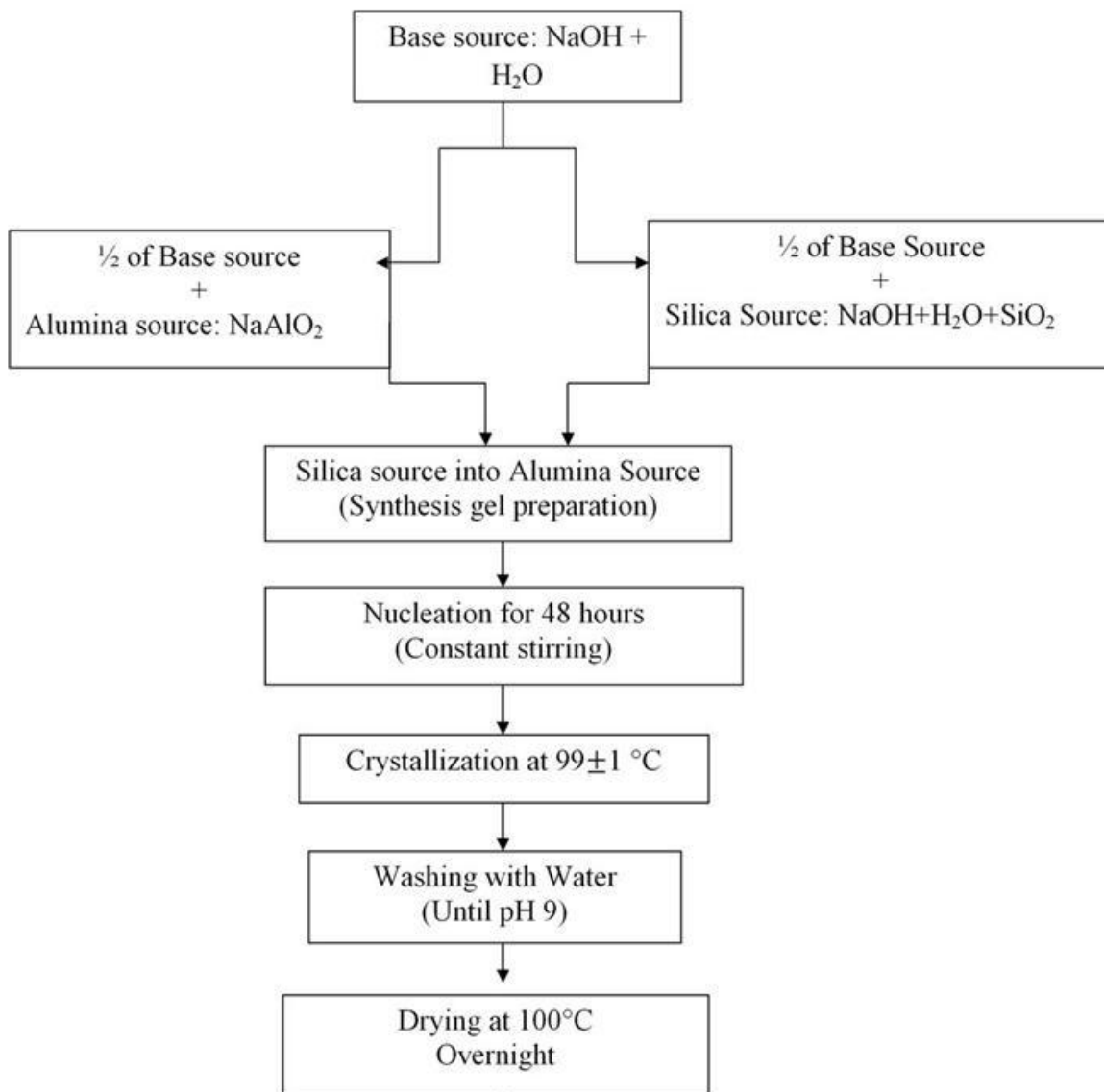


Figure 3.1: synthesis steps for Na-P1 Zeolite

3.2 Synthesis of DAC-Na

Experimental

Reactants used for this work was as follows: Silica source was Tetraethylorthosilicate (98% Aldrich), Alumina source was sodium aluminate (anhydrous, Sigma-Aldrich) while Tetraethyleammonium hydroxide (40% in H₂O, Aldrich) and Tetrapropylammonium bromide (98%, Aldrich) were used as double structure directing agents. While water source used was ultra pure water. All reactants were used in this molar ratio: 29TEOS: NaAlO₂:10TEAOH:8TPABr:850 H₂O

Process Details

The main objective was to obtain nanocrystalline zeolite in reflux flask by mean of introducing organic template in the reactants system. The stepwise description of each operation is described below:

1. Synthesis solution preparation

Sol 1: 18.4ml of TEAOH (Tetraethyl ammoniumhydroxide) was mixed with 73.4ml of ultra pure water in a conical flask following by slow addition of 0.4g of sodium aluminate. Under constant mixing with the help of magnetic stirrer at 100 rpm, white solution turned into colorless. Its pH was noted to be 12.9.

Sol 2: 29ml TEOS (tetraethylorthosilicate) was poured into another flask followed by slow addition of 10.9g TPABr (tetrapropyl ammoniumbromide). It was vigorously mixed with electric stirred until completely mixed.

Solution preparation: Then sol 2 was poured into sol 1, as a result clear solution was prepared under constant stirring (electric stirrer).

2. Nucleation

The solution was mixed under the same parameter for 48 hours.

3. Rotary evaporation

After completion of nucleation time, it was necessary to remove alcohols produced during constant mixing; they were evaporated at 50°C, 100rpm, for 20 minutes. Vacuum pressure applied was 40kPa. In the end 50% solution by volume was separated from the original solution and was supposed to be alcoholic medium.

4. Crystallization

The purified solution was shifted to round bottom flask and introduced into a total reflux setup. Solution was heated up to 65±5 °C while constantly stirring at 200 rpm (this time it was done with magnetic stirrer). Crystallization time was different for different experiments; the process was repeated for six times to collect samples for crystallization time of 12, 24, 36, 48, 60 and 72 hours.

5. Centrifugation

Centrifugation at 14000 rpm for 15 minutes separated solid from liquid. Solid containing zeolite crystals having pH 9 were shifted into washing unit.

6. Washing

All samples were washed immediately, with cold Ultra pure water until remaining pH was up to 7.9.

7. Drying

After washing, samples were introduced into air oven, while heating at 100 °C for whole night.

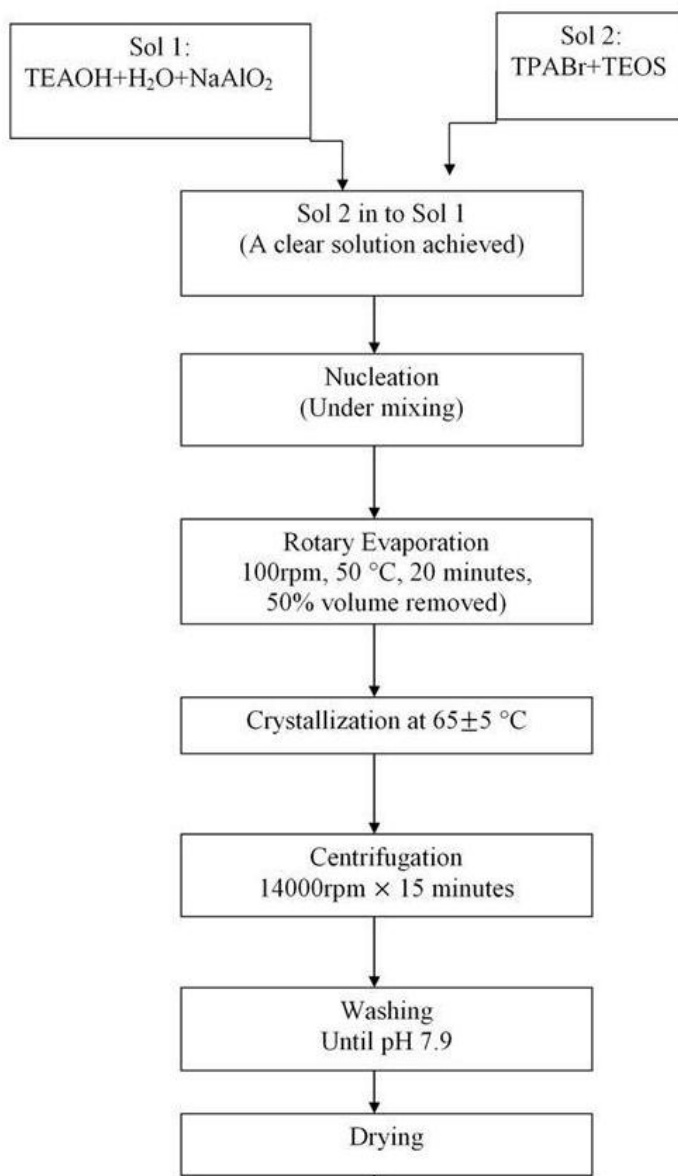


Figure 3.2: synthesis steps for DAC-Na Zeolite

Chapter 4: Results and Discussion

4.1.1 XRD for Na-P1 Zeolite

The result obtained for Na-P1 zeolite is expressed in figure 4.2. Sample A1 (12 hours) is showing one dimensional growth of Na-P1 crystals that keep on improving for A2 (14 hours), A3 (16 hours). Sample A4 (18 hours) showing removal of all extra framework structures and tends to the formation 3D crystals growth. Sample A5 shows formation of cubical crystals of Na-P1 but still it has extraframework structure. It might show that with the passage of time, continuous heating at 100°C under constant stirring force the synthesis gel to grow in a single crystal structure.

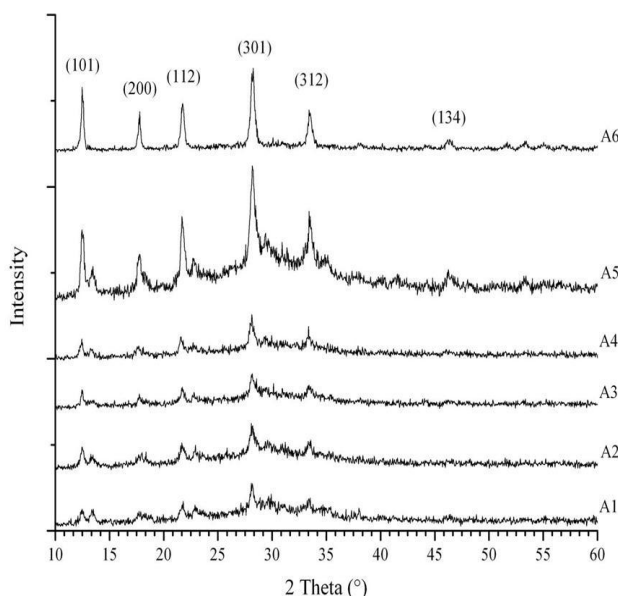


Figure4.2: XRD results for Na-P1 zeolite; where A1 (12 hours); A2 (14 hours); A3 (16 hours); A4 (18 hours); A5 (20 hours); A6 (22 hours) Here, peak list, detected and matched by software was double checked by collection of simulated XRD powders^[68]; published on behalf of the Structure Commission of the International Zeolite Association. Table 4.1 shows assignment of peaks for sample A6.

Peak Position (°)		FWHM (β)		$\tau = \frac{K\lambda}{\beta \cos \theta}$
2theta	theta	2theta	Radian	Crystal size (nm)
12.49	6.24	0.2	0.0017	83.3
17.75	8.87	0.2	0.0017	83.3
21.74	10.87	0.28	0.0024	59.3
28.20	14.10	0.24	0.0020	72.1
33.45	16.72	0.16	0.0013	112.4

Table 4.1: Na-P1 XRD assignments
K: shape factor = 0.94 radian
 λ : X-Ray wavelength = 0.154 nm

4.1.2 XRD for DAC-Na zeolite

Figure 4.3 expresses the XRD analysis results for DAC-Na type zeolite. Showing that B1 (12 hours) was almost amorphous aluminosilicate gel when heated at $65\pm 5^\circ\text{C}$ under constant stirring, and no special affect observed in B2 (24 hours). However B3 (36 hours) and B4 (48 hours) showed significant crystal growth that became prominent for B5 (60 hours). B6 (72 hours) show dominance of monoclinic crystal structure of DAC-Na zeolite. Digital peaks indication and matching was performed by using X'pert Highscore and then verified by collection of simulated XRD powders^[68]; published on behalf of the Structure Commission of the International Zeolite Association. The result showing peak intensity was different from that of simulated pattern for DAC-zeolite. This indicates the anisotropic tendency of our synthesized product. Another phenomena observed during crystallization was “lower temperature leads to the formation of nanocrystalline zeolite”. Crystal size for B6 was lesser than B5. The reason might be the low temperature crystallization. That might have consumed more time to synthesize DAC-Na but smaller crystals achieved.

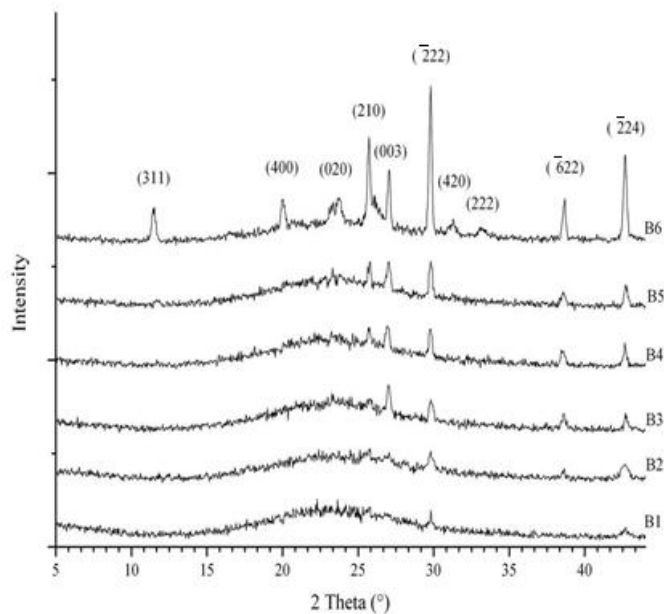


Figure4.3: XRD results for DAC-Na zeolite; where B1 (12 hours); B2 (24 hours); B3 (36 hours); B4 (48 hours); B5 (60 hours); B6 (72 hours)

Peaks assignments were performed using the same source as for Na-P1 zeolite. Table 4.2 expresses the XRD details for sample B6.

Peak Position (°)		FWHM (β)		$\tau = \frac{K\lambda}{\beta \cos \theta}$
2theta	theta	2theta	Radian	Crystal size (nm)
11.44	5.72	0.1574	0.0014	100
19.96	9.98	0.1968	0.0015	94.7
23.73	11.86	0.2362	0.002	71.5
25.71	12.85	0.1574	0.0014	102.5
27.06	13.53	0.1574	0.0014	102.8
29.80	14.9	0.1968	0.0015	96.5
31.24	15.62	0.4723	0.004	36.3
33.32	16.66	0.9446	0.008	18.26
38.65	19.32	0.275	0.002	74
42.67	21.33	0.236	0.002	75

Table 4.2: DAC-Na XRD assignments
K: shape factor = 0.94 radian; λ : X-Ray wavelength = 0.154 nm

4.2.1 SEM Analysis for Na-P1

Na-P1 type samples were dispersed in isopropyl alcohol in ultra sonic bath for 20 minutes, sample holder was laminated with copper foil, and sample was dropped. After evaporation of isopropyl alcohol from the sample, Gold was sputtered on the sample and it was introduced to SEM analysis. Following diagram contains stacked images of P type material crystallized for various hours; showing initially needles were grown from zeolite crystals, that when exposed to more time for crystallization, generating the porous cubic aggregates of Zeolites.

Figure 4.4 expresses the stacked results for Na-P1 SEM analysis.

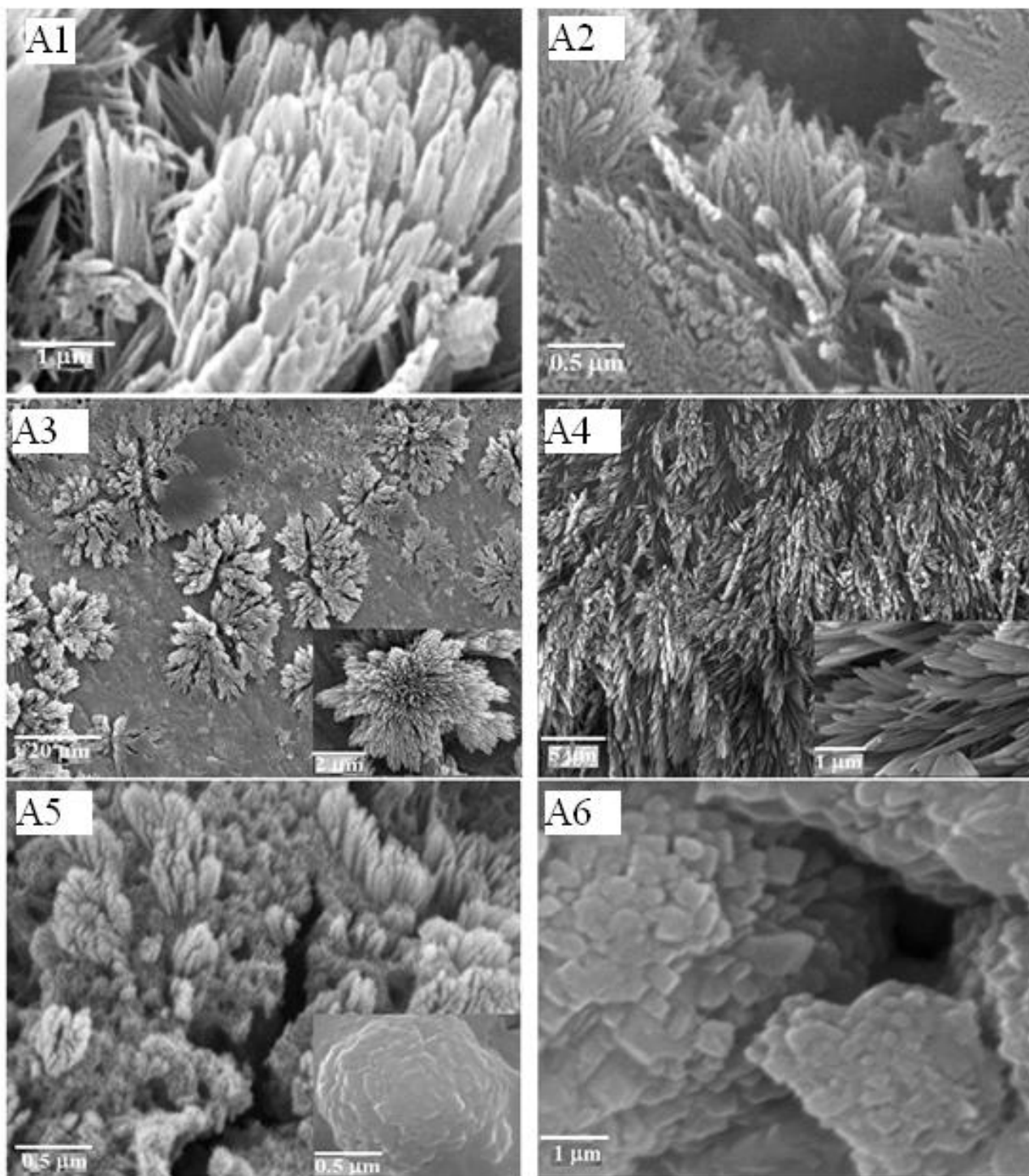


Figure 4.4: SEM analysis for Na-P1

4.2.2 SEM Analysis for DAC-Na

DAC-Na type samples were dispersed in isopropyl alcohol in ultra sonic bath for 20 minutes, sample holder was laminated with copper foil, and sample was dropped. After evaporation of isopropyl alcohol from the sample, Gold was sputtered on the sample and it was introduced to SEM analysis. Following diagram contains stacked images of B type material crystallized for various hours; dictating that for this much lower temperature of crystallization, initially crystals were agglomerated and under constant stirring, they started to get dispersed in smaller size, as shown in the SEM results (Figure 4.5).

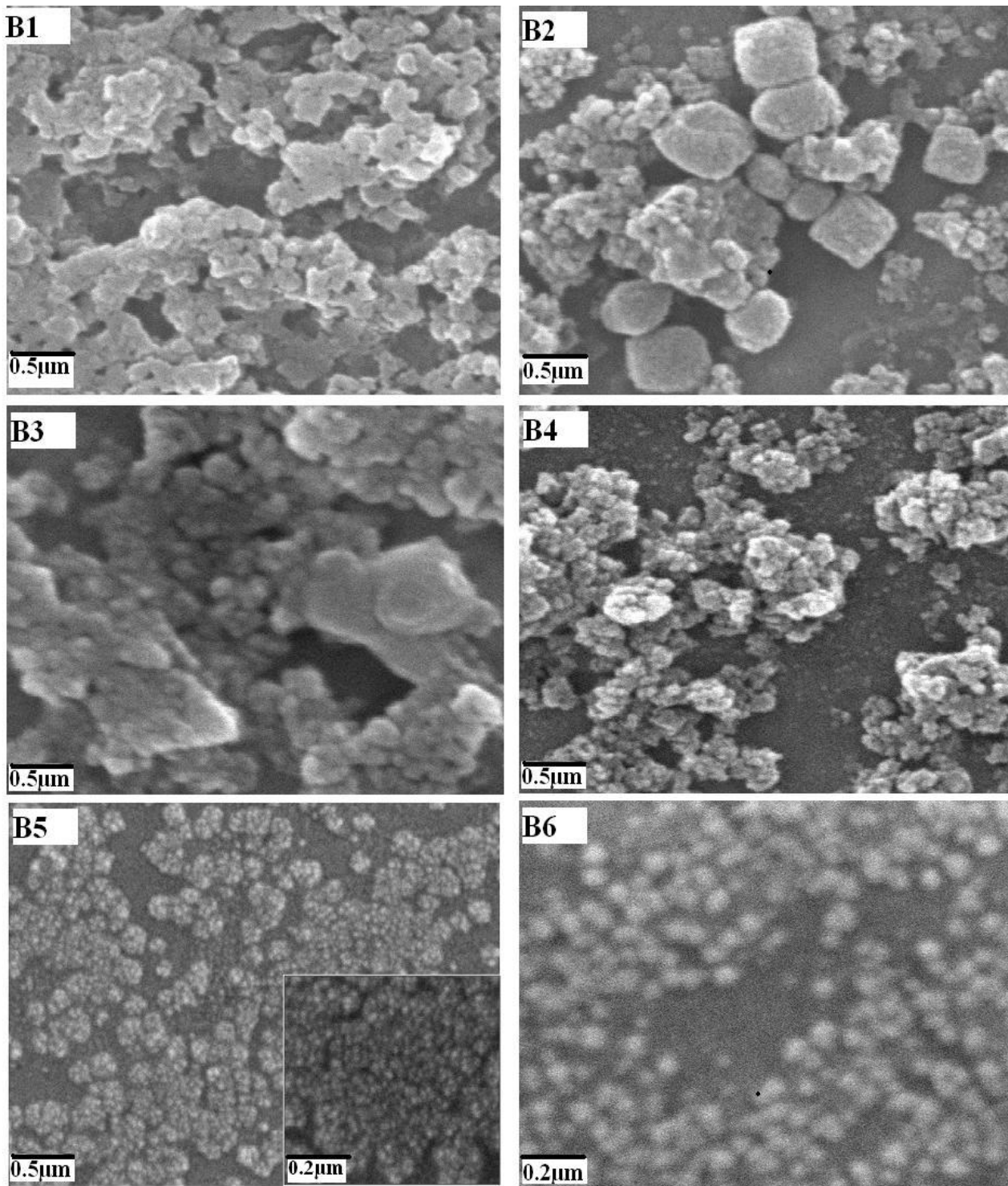


Figure 4.5: SEM analysis for DAC-Na

4.3.1 AFM Analysis for Na-P1

Dispersion was made in isopropyl alcohol while sonication for 30 minutes in ultra sonic bath, final dispersed sample was dropped on sample holder coated with graphite. Result (figure 4.6 and 4.7) show that small aggregates for Na-P1 cubes were formed when crystallization was performed for A6 (22 hours).

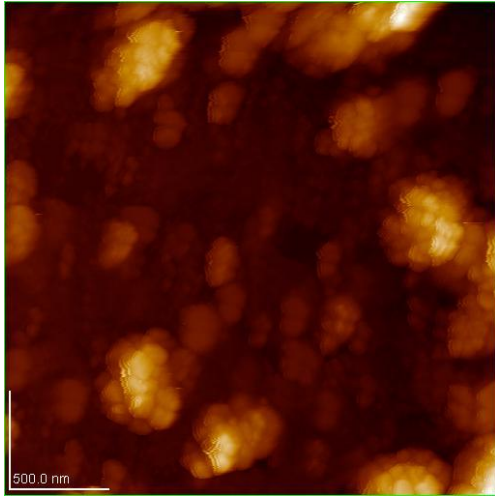


Figure 4.6: AFM result for Na-P1 (2-dimensional)

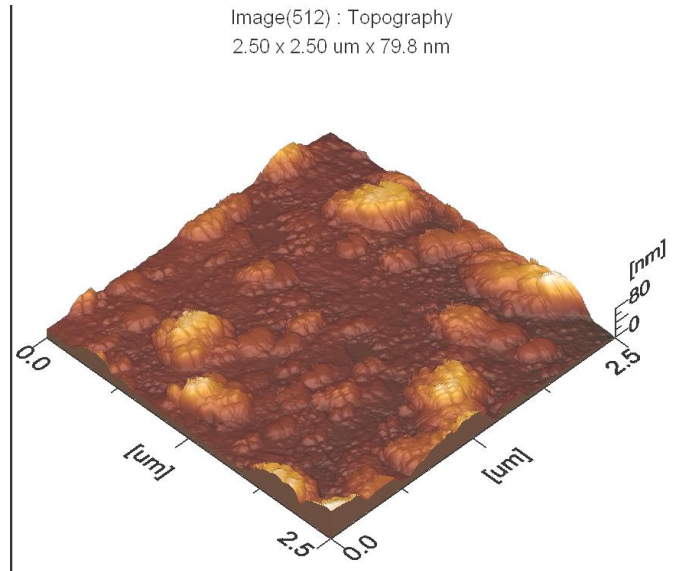


Figure 4.7: AFM result for Na-P1 (3-dimensional)

Particle size distribution for Na-P1 measured during AFM analysis indicated that most of Na-P1 was aggregated of size 30 nm (figure 4.8).

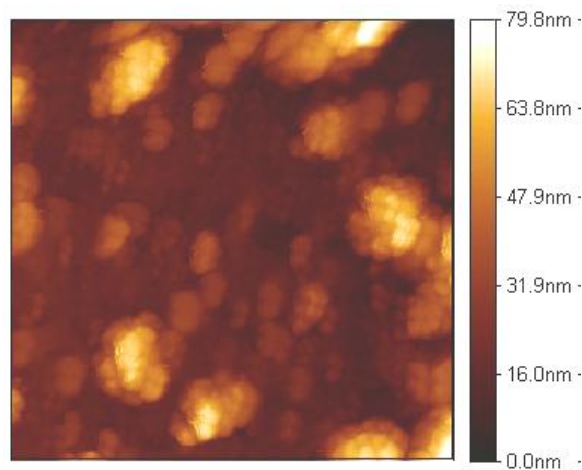


Figure 4.8: AFM Analysis: Particle size distribution for Na-P1 zeolite

4.3.2 AFM Analysis for DAC-Na

Dispersion was made in isopropyl alcohol while sonication for 30 minutes in ultra sonic bath, final dispersed sample was dropped on sample holder coated with graphite. Result (figure 4.9 and 4.10) show that small aggregates for DAC-Na were formed when crystallization was performed for B6 (72 hours).

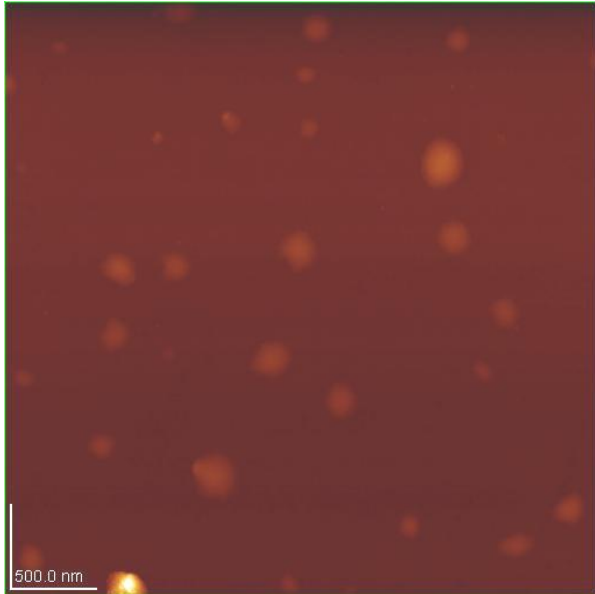


Figure 4.9: AFM result for DAC-Na (2-dimensional)

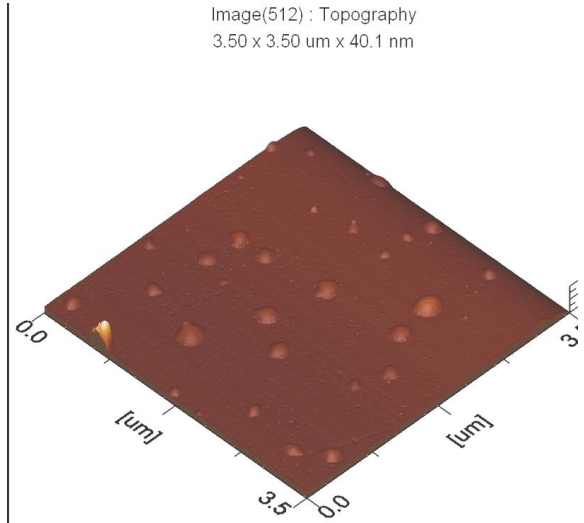


Figure 4.10: AFM result for DAC-Na (3-dimensional)

Particle size distribution for DAC-Na measured during AFM analysis indicated that most of DAC-Na was aggregated of size 16 nm (figure 4.11).

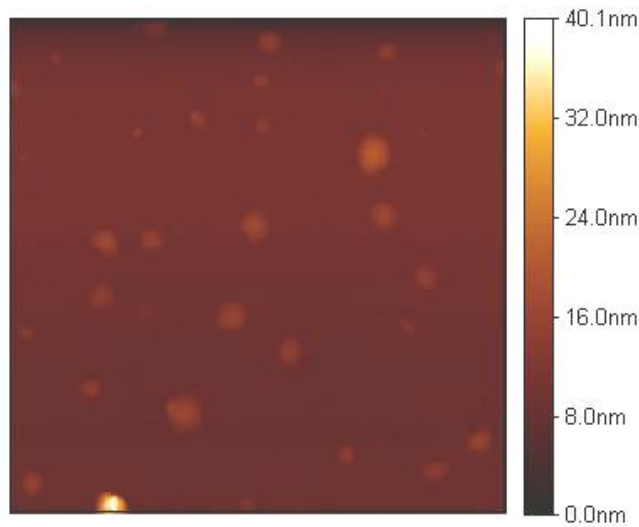


Figure 4.11: AFM Analysis: Particle size distribution for DAC-Na zeolite

4.4 FT-IR Analysis

Initially, FT-IR spectra analysis was used to interpreting absorption bands as functional groups of sample materials for both amorphous and crystalline microstructured solids.^[70-73] however, functional groups of liquids as well as nanostructured materials are also characterized through the same technique.^[74] A routine sample preparation for FT-IR analysis is the preparation of small, round pellets in hydraulic press machine after mixing finely grinded 99% KBr and 1% solid sample material. As a result, transparent pellet casted is introduced to machine where IR rays pass through it and generate absorption bands when graph is plotted between %transmittance and wavenumber (cm^{-1}). We used Perkin Elmer PE 1600 FTIR machine to characterize our sample. The FT-IR spectra of sample A5 for Na-P1 type material as shown in figure 4.12, shows seven major absorption bands:

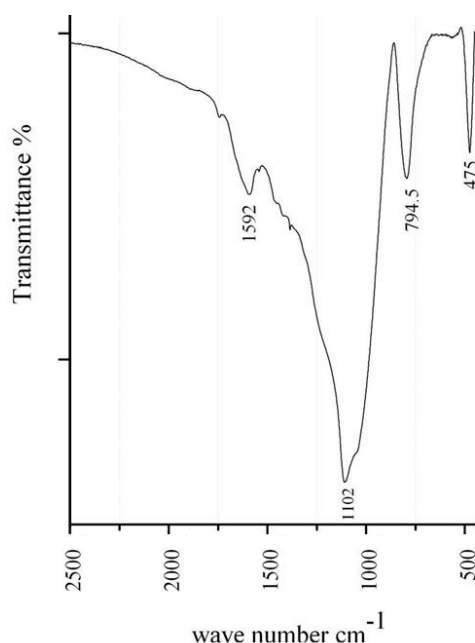


Figure 4.12: FT-IR result for Na-P1 (A5) transmission mode

The absorption band (medium) at 1592 is assigned to the bending mode of Na-group.^[75] The medium band between 1600 cm^{-1} and 1500 cm^{-1} can be attributed as the sodium ions attached around zeolitic framework. The band at 1102 cm^{-1} (very strong) is assigned to asymmetric bending modes of TO_4 silicate groups (T can be Si or Al). while bands at 794.5 cm^{-1} indicates symmetric bending modes of TO_4 group. Similarly bands at 475 cm^{-1} are associated with TO_4 tetrahedra of silicate and aluminate groups.

Chapter 5: Application

A Comparative Study of Thermal and Catalytic Pyrolysis of LDPE

5.1 Thermogravimetric Study of LDPE Pyrolysis with Na-P1

For Thermogravimetric study of LDPE pyrolysis with Na-P1, TGA was performed by “Diamond TGA/DTA (Thermogravimetric/Differential thermal analyzer), Perkin Elmer instruments. Heat flow rate was set to 10°C/min by using Argon as purge gas. LDPE pellets with an average size of 5mm were purchased from Diamond Scientific Store (Rawalpindi, Pakistan). The physical properties of the LDPE pellets were a melting point of 110°C, a melt flow index of 0.3g/10min, and a density of 0.92g/cm³. Pyrolysis of LDPE with Na-P1 (figure 5.1) shows that pure LDPE (Black line) do not shows any decomposition from 30°C to 430°C. From 430°C to 500°C, pure LDPE shows decomposition, after which no weight loss observed. So thermal pyrolysis of pure LDPE shows total weight loss of 72%. Possibly wax contents having 28% of initial weights are residuals left behind. When 5% of Na-P1 mixed with pure LDPE (Red line), it TGA analysis shows that weight loss occurred in three segments. First 280-340°C, then 340-400°C and then 400-470°C, this curve shows (red line), total weight loss observed was 78%. So possible wax contents, left behind at the end of experiment were 22%. When 3% Na-P1 was mixed with LDPE, TGA (green line) shows decomposition occurs from 400-490°C, where total weight loss observed is 85%. So possible wax contents, left behind at the end of experiment were 15%. When 2% Na-P1 was mixed with LDPE, TGA (blue line) shows decomposition was almost similar to that of green line (3% Na-P1), but analysis showed total weight loss for sample was 84%. So possible wax contents, left behind at the end of experiment were 16%. This is very important factor for pyrolysis that how less residuals are left behind. So using 2% Na-P1 resulted in less residual contents observed in the end of pyrolysis. Table 5.1 shows the summary of Thermogravimetric study of LDPE pyrolysis with Na-P1.

Sample	Decomposition temperature ranges	Residual weight
Pure LDPE	430°C to 500°C	28%
LDPE with 5%Na-P1	280-340°C 400-470°C	22%
LDPE with 3% Na-P1	400-490°C	15%
LDPE with 2% Na-P1	400-490°C	14%

Table 5.1: Thermogravimetric study of LDPE pyrolysis with Na-P1

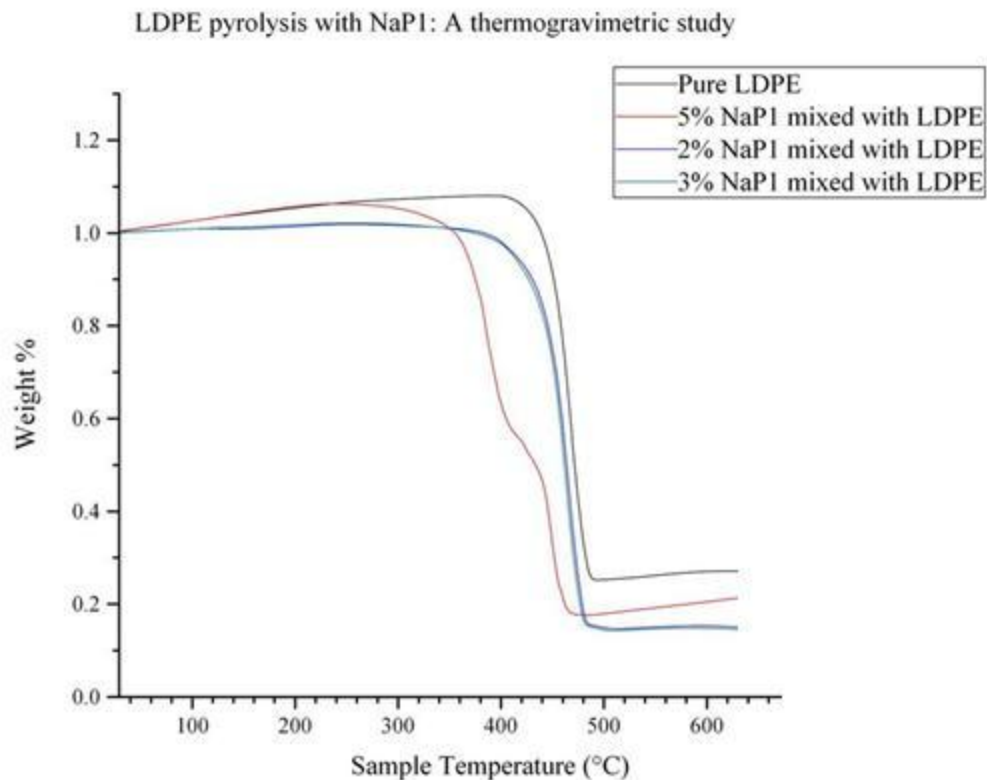


Figure 5.1: Thermogravimetric study of LDPE pyrolysis with Na-P1

5.2 Thermogravimetric Study of LDPE Pyrolysis with DAC-Na

For Thermogravimetric study of LDPE pyrolysis with DAC-Na, TGA was performed by “Diamond TGA/DTA (Thermogravimetric/Differential thermal analyzer), Perkin Elmer instruments. Heat flow rate was set to 10°C/min by using Argon as purge gas. LDPE pellets with an average size of 5mm were purchased from Diamond Scientific Store (Rawalpindi, Pakistan). The physical properties of the LDPE pellets were a melting point of 110°C, a melt flow index of 0.3 g/10min, and a density of 0.92g/cm³. Pyrolysis of LDPE with DAC-Na (figure 5.2) shows that pure LDPE (Black line) do not shows any decomposition from 30°C to 430°C. From 430°C to 500°C, pure LDPE shows decomposition, after which no weight loss observed. So thermal pyrolysis of pure LDPE shows total weight loss of 72%. Possibly wax contents having 28% of initial weights are residuals left behind. When 5% of DAC-Na mixed with pure LDPE (Red line), it TGA analysis shows that weight loss occurred in three segments. First 300-390°C, then 390-460°C and then 460-480°C, this curve shows (red line), total weight loss observed was 82%. So possible wax contents, left behind at the end of experiment were 18%. When 3% DAC-Na was mixed with LDPE, TGA (green line) shows decomposition occurs from 380-475°C, where total weight loss observed is 76%. So possible wax contents, left behind at the end of experiment were 24%. When 2% DAC-Na was mixed with LDPE, TGA (blue line) shows decomposition

occurs from 360-475°C, where total weight loss observed is 80%. So possible wax contents, left behind at the end of experiment were 20%. This is very important factor for pyrolysis that how less residuals are left behind. Table 5.2 shows the summary of Thermogravimetric study of LDPE pyrolysis with DAC-Na. So using 5% DAC-Na resulted in less residual contents observed in the end of pyrolysis.

Sample	Decomposition temperature ranges	Residual weight
Pure LDPE	430°C to 500°C	28%
LDPE with 5% DAC-Na	300-390°C 460-480°C	18%
LDPE with 3% DAC-Na	380-475°C	24%
LDPE with 2% DAC-Na	360-475°C	20%

Table 5.2: Thermogravimetric study of LDPE pyrolysis with Na-P1

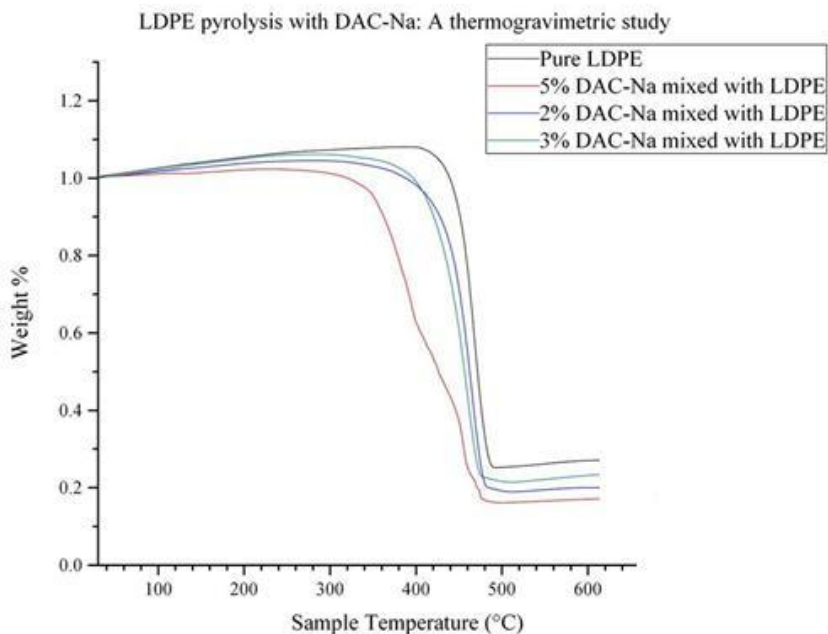


Figure 5.2: Thermogravimetric study of LDPE pyrolysis with DAC-Na

Chapter 6: Future Work:

Zeolites are versatile materials, industrial gas absorption, ion-exchange, drug carrier, catalysis are various applications. Future work for present work can be:

1. Altering synthesis recipe to prepare products with various silica to alumina ratio to investigate their catalytic activity and influence of crystal size on catalysis.
2. Ion-exchange of Na-P1 and DAC-Na with Hydrogen ion and other metals to investigate catalytic activity over various petrochemical reactions.
3. Calcium absorption capability of Na-P1 can make it considerable candidate for detergent composition.
4. Absorption of heavy metals from industrial waste effluents to improve environment.

Chapter 7: Conclusion

Nanocrystalline Na-P1 zeolite (~ 70 nm) was successfully synthesized using hydrothermal reflux method. Nanocrystalline DAC-Na of crystallite size ~ 20 nm was synthesized using reflux method. Catalytic pyrolysis of LDPE: Initial experiments showed that the above mentioned catalysts were better cracking catalysts.

References

- [1] Staff Report, *Pakistan Today, Pakistan*. March 19, 2012.
- [2] *Historical Dictionary of the Petroleum Industry*. Vassiliou, Marius. Scarecrow Press, 2009, 700.
- [3] *Natural and Synthetic Zeolites*. U.S. Bureau of Mines Information Circular, 1987, 9140.
- [4] *Handbook of zeolite science and technology*, Scott M. Auerbach, Kathleen A. Carrado, Prabir K. Dutta, eds. CRC Press, 2003, 16.
- [5] *Zeolites (natural)*, USGS Mineral Commodity Summaries 2011.
- [6] *Heterogeneous asymmetric epoxidation of cis-ethyl cinnamate over Jacobsen's catalyst immobilized in inorganic porous materials*, Rihakova, Y.L. Thesis, 2010, 31.
- [7] *W. R. Grace & Co. Enriching Lives, Everywhere. – Zeolite Structure*. Grace.com. 2010.
- [8] Schoonover, M.W.; Cohn, M.J. *Top Catal.* 2000, 13, 367–370.
- [9] Davis, M.E. *Ind. Eng. Chem.* 1991, 30, 1675.
- [10] *Framework Type DAC, Database of zeolite structures, Structure Commission of the International Zeolite Association*
(http://izasc.ethz.ch/fmi/xsl/IZA-SC/ftc_main_image.xsl?db=Atlas_main&-lay=fw&STC=DAC&-find)
- [11] Meier, W.M.; Baerlocher, C. *Zeolite Type Frameworks, Springer-Verlag Berlin Heidelberg*, Vol. 2, 1999.
- [12] Ed: Catlow, C. R. A. *Modeling of Structure and Reactivity in Zeolites. Academic Press, Ltd.: London*. 1992.
- [13] Burkett, S. L.; Davis, M.E. *J. Phys. Chem.* 1994, 98, 4647.
- [14] Kirschhock, C. E. A.; Ravishankar, R.; Loooveren, L. V.; Jacobs, P.A.; Martens, J.A. *J. Phys. Chem.* 1999, 103, 4972.
- [15] Harris, T.V.; Zones, S.I. *Stud. Surf. Sci. Catal.* 1994, 29, 94.
- [16] Zones, S.I.; Santilli, D.S. *Proc. Ninth Int. Zeolite Conf.*, ed. Ballmoos, R.V.; Higgins, J.B.; Treacy, M.M.J. Butterworth-Heinemann, Boston, MA. 1993, p.171.
- [17] Lobo, R.F. et al. *J. Phys. Chem.* 1994, 98, 12040.
- [18] Schmitt, K.D. et al. *Zeolites*. 1994, 14, 635.
- [19] Fyfe, C.A. et al. *J. Phys. Chem.* 1990, 94, 3718.
- [20] Dove, P.M. et al. *Geochim. Cosmochim. Acta*. 1990, 54, 955.
- [21] Slangen, P.M.; Jansen, J.C.; Van Bekkum, H.; *Microporous Mater.* 1997, 9, 259-265.
- [22] Freund, E.F.; *J. Cryst. Growth*, 1976, 34, 11-23.
- [23] Barrer, R.M.; *Hydrothermal Chemistry of Zeolites*, Academic Press Inc., London, 1982.
- [24] Davis, M.E.; Lobo, R.F.; *Chem Mater.*, 1994, 4, 756-768.
- [25] Barrer, R.M.; *Hydrothermal Chemistry of Zeolites*, Academic Press Inc., London, 1982.
- [26] James H. G.; Glenn E. H. *Petroleum Refining: Technology and Economics*. CRC Press. 2001,4.
- [27] *Natural and Synthetic Zeolites*. U.S. Bureau of Mines Information Circular. 1987, 9140.
- [28] Li, X.; Li, C.; Zhang, J.; Yang, C.; Shan, H. *J. Natural Gas Chemistry* 2007, 16, 92-99.
- [29] Subbiah, A. C., Byong K.; Blint, Richard J.; Gujar, Amit; Price, Geoffrey L.; Yie, Jae E. *Applied Catalysis, B: Environmental*. 2003, 42, 155-178.
- [30] Guisnet, M. *Methods and Reagents for Green Chemistry*. 2007, 231-249.
- [31] Larsen, S. C. *J. Phys. Chem.* 2007, 111, 18464-18474.
- [32] Ando et al. *United states Patent*, Patent No. US 6692722, feb. 17,2004.

- [33] Anton, P., Jasmine, F. and Sarah C. L. *Langmuir*. 2010, 26(9), 6695-6701.
- [34] Elodie, B. L.; Francois, F.; Didier, A. *Thierry Des Courieres Microporous Materials*. 1993, 1, 237-245.
- [35] Baerlocher, Ch.; Meier, W.M. *Z. Kristallogr.* 1972, 135, 339-354.
- [36] Breck, W.D.; Eversole, W.G.; Milton, R.M. *J. Am. Chem.Soc.* 1956, 78, 2338.
- [37] Barrer, R.M.; Baynhan, J.W.; Bultitude, F.W.; Meier, W.M. *J. Chem. Soc.* 1959, 195.
- [38] Regis, A.J.; Sand, L.B.; Calmon, M.E. G., *J. Phys. Chem.* 1960, 64, 1567.
- [39] Milto, R.M. *US Patent 3,008,803*, 1961.
- [40] Barrer, R.M.; Baynhan, J. W.; Bultitude, F.W.; Meier, W.M. *J. Chem. Soc.* 1959, 195.
- [41] Baerlocher, Ch.; Meier, W.M. *Z. Kristallogr.* 1972, 135, 339.
- [42] Hansen, S.; Hakanson, V. Falth, L. *Acta Crystallogr.* 1990, 46, 1361.
- [43] Baerlocher, Ch.; Meier, W.M.; Olson, D.H. *Atlas of the Zeolite Structure Types*, Elsevier, Amsterdam. 2001, 5.
- [44] Gottardi, G.; Galli, E. *Natural Zeolites*, Springer-Verlag, Berlin. 1985, 157.
- [45] Taylor, A.M.; Roy, R. *J. Chem. Soc.* 1965, 4028.
- [46] Taylor, A.M.; Roy, R. *Am. Miner.* 1964, 49, 656.
- [47] Hansen, S.; Landas-Canovas, A.; Hakanson, U. L. *Falth, Zeolites*. 1993, 13, 276.
- [48] Beard, W.C. *Adv. Chem. Ser.* 1971, 101, 237.
- [49] Alberti, A.; Vezzalini, G. *Acta Cryst.* 1979, 35, 2866.
- [50] Arkadiusz, D.; Marek, M. *Mineralogia Polonca Doi*, 2007, 38, 1.
- [51] Dusica, V.; Igor, M.; Aleksandarrosi, A.; Predrag, L. *J.Serb.Chem.Soc.* 2003, 68, 471-478.
- [52] Mouhtar, Th. et al. *Tsira. Micro. Meso. Mater.* 2003, 61, 57-67.
- [53] Querol, X. et al. *Geologica Acta*. 2007, 5, 49-57.
- [54] Adamczyk, Z.; Bialecka, B. *Pol. J. Env. Stud.* 2005, 14, 713-719.
- [55] Zouboulis, A.I.; Goultonas, A. *Fresen. Environ. Bull.* 1995, 4, 387.
- [56] Adams, C.J. et al. *J. Chem. Soc. Faraday Trans.* 1997, 93, 499.
- [57] Jeong-Geol, N.A. et al. *J Mater Cycles Waste Manag*, 2006, 8, 126-132.
- [58] Adams, C.T. et al. *US5560829A*. Oct. 1, 1996.
- [59] Abraham, A. *US006258768B1*. Jul. 10, 2001.
- [60] Junhang, D.; Lin, Y.S. *Ind. Eng. Chem. Res.* 1998, 37, 2404-2409.
- [61] Jeong-Geol, N.A. *J Mater Cycles Waste Manag*. 2006, 8, 126-132.
- [62] Coombs, D.S. et al. *Rec Z Min.* 1997, 35, 1571-1606.
- [63] Gottardi, G.; Meier, W.M. *Z. Kristallogr.* 1963, 119, 53-64.
- [64] Bonardi, M. et al. *Quebec. Can. Min.* 1981, 19, 285-290.
- [65] Hayim, A. *US 2005/0130832 A1*, Nov 17, 2004.
- [66] Tracy, J. H. et al. *US 4339606*, July 13, 1982.
- [67] Pecharsky, V. K.; Zavalij, P. Y., *Fundamentals of powder diffraction and structural characterization of materials*. New York: Springer, 2005.
- [68] *XRD Powder Patterns for Zeolites*; Ed: M.M.J. Treacy and J.B. Higgins; Elsevier. 2001, 4.
- [69] Patterson, A. L. *Physical Reviews*. 1939, 56, 978-982
- [70] von Ardenne, *Manfred für Physik*. 1939, 109, 553-572.
- [71] Nyquist, R.A. et al. *Infr Spec Ino Cos*, Academic Press Inc., New York, 1973, 495.
- [72] Shigemoto, N. et al. *J. Mater. Sci.* 1995, 30, 5777.
- [73] Hawthorne, F. *Can. Mineral.* 1993, 31, 253.

- [74] Godelitsas, A. et al. in: Pro 7th Con,Thessaloniki, Bull. Geol. Soc. Greece, 1994, 3, 301.
- [75] Putnis, A. *Intro Min Sci, Cambridge University Press.* 1992, 479.
- [76] Godelitsas, A. et al. in: Pro 7th Con,Thessaloniki, Bull. Geol. Soc. Greece, 1994, 3, 301.
- [77] Fordham, C.J.; Smalley, I.J. *Cent. Concr.* 1985, 15, 141.
- [78] Chandra, S.; Flodin, P. *Inter Por Cem Hyd. Cement Concrete Research.* 1990, 17, 975-890
- [79] Ollitrault-Fichet, R. et al. *Cement and Concrete Research.* 1998, 12, 1687-1693.
- [80] Tisivilis, S. et al. *Journal of thermal analysis.* 1998, 52, 863-870.
- [81] Dweck, C.S. et al. *Self-theories:Their Role in Motivation. Psychology Press, Philadelphia.* 2000.
- [82] Dennis, M. *Intr. Ind. Polye: Pro, Cat, Pros. John Wiley and Sons.* 2010, 1.
- [83] <http://www.ceresana.com/en/market-studies/plastics/polyethylene-ldpe/>
- [84] Jan, K. *The News, Pakistan.* December 13, 2011
- [85] Haris, H. *Daily Times, Pakistan.* January 02, 2012
- [86] Mayra, I. *The News, Pakistan.* April 25, 2011,
- [87] Ali, M. F.; Qureshi, M. S. *African J. Pure App. Chem.* 2011, 9, 284-292.
- [88] Lopez-Uriónabarrenechea, A. et al. *J. Ana. App. Pyr.* 2012, 96, 54–62.
- [89] Pandian, S.; Kamalakannan, A.; *Int. J. Chem. Res.* 2012, 3.
- [90] Behja, T. *European. J. Sci. Res.* 2009, 32, 223-230.
- [91] Kyong-Hwan, L. et al. *Korean J. Chem. Eng.* 2003, 20, 693-697.
- [92] Jeong-Geol, N.A. et al. *J. Mater. Cycles. Waste Manag.* 2006, 8, 126–132.